The Dissertation Committee for Vita Marie Vock certifies that this is the approved version of the following dissertation:

Evidence for muscle-dependent neuromuscular synaptic site determination in mammals

Committee:

Mendell Rimer, supervisor

Wesley Thompson, co-supervisor

Seema Agarwala

Bing Zhang

Kevin Dalby

Evidence for muscle-dependent neuromuscular synaptic site determination in mammals

by

Vita Marie Vock, B.S.

Dissertation

Presented to the Faculty of the Graduate School of

The University of Texas at Austin

in Partial Fulfillment

of the Requirements

for the Degree of

Doctor of Philosophy

The University of Texas at Austin

December 2007

Dedication

I dedicate this dissertation to my wonderful children Justin, Ryan and Alanna. Thank you all for giving me a reason to keep striving, and the courage to reach out for my dreams. You will ever be my inspiration.

Acknowledgements

My sincere gratitude to Mendell Rimer for his mentoring, support and guidance. Thanks to Lewis Chodosh, Tom Jessell, Steve Burden and Wes Thompson for providing the breeding pairs for tetO-CAErbB2+/-, Hb9+/-, and S100-GFP mice, respectively, and to Steve Burden for the plasmid probes for in-situ hybridization. Thanks to my committee members for their patience and diligent oversight, and to my good friend Anita Latham, for her unending encouragement. Thanks to previous research mentors, notably Audrey Atkin who provided a sound foundation for my lab skills. My thanks to Audrey Atkin, Miles Wilkinson and Mendell Rimer for recognition of my potential. Many thanks to Shan Maika and Angela Bardo for their technical assistance, and to John Mihic and Richard Aldrich for their advice, guidance and encouragement. Special thanks to Elaine Ellerton and Olga Ponomareva for providing a lab environment where I wanted to be, and to the INS students for creating a fantastic peer group. Personal thanks to the jewish group for truly being like family. Thanks to my parents for not asking too many questions and to my siblings for their pride. My very special thanks to my children and loving husband for believing in me, for providing motivation, and for constantly tolerating my ridiculous puns, meshugas, and hours of trashy television. Thanks also to my amazing puppy DJ for being the best cancer therapy anyone could ever hope for.

Evidence for muscle-dependent neuromuscular synaptic site determination in mammals

Vita Marie Vock, Ph.D.

The University of Texas at Austin, 2007

Supervisors: Mendell Rimer and Wesley Thompson

Recent evidence has challenged the prevalent view that neural factors induce the formation of a de novo postsynaptic apparatus during development of the vertebrate neuromuscular junction. The latest experiments suggest an alternative, muscle-dependent model in which the muscle induces the nascent postsynaptic apparatus and sets the location of the future synapse. Once contacted by the incoming axons, these sites, laid out in a pre-pattern in the central area of developing muscle fibers, mature into synapses by the combined action of neural factors such as agrin and ACh. In this study, I sought to provide a test in mammals for these two models of neuromuscular synaptogenesis. Previously, our laboratory showed that continuous muscle expression of constitutively active ErbB2 (CAErbB2) during embryogenesis leads to synaptic loss, exuberant axonal sprouting and lethality at birth. Here, I transiently induced CAErbB2 during midgestation

and examined the process of synapse restoration after inducer withdrawal. Centrally-enriched AChR transcription and AChR clustering were abolished as a result of transient CAErbB2 induction. After inducer withdrawal, synapses were restored but were distributed widely over the entire surface of the diaphragm. Under the nerve-dependent model, this distribution would have been explained by the wide pattern of axonal sprouting triggered by CAErbB2 expression. Yet, in the absence of the nerve, introduced in our transgenic animals by mating to Hb9+/- mice, a very similar, wide distribution of aneural AChR clusters was generated. Thus, even in a case where the central pre-pattern of AChR transcription and clustering is missing, it is the muscle, and not the nerve, that seems to set the site for synapse formation. My results support a muscle-dependent model for the induction of neuromuscular synaptogenesis in mammals.

Table of Contents

List of Figures

CHAPTER 1

Introduction

STRUCTURE OF THE NEUROMUSCULAR JUNCTION

The vertebrate neuromuscular junction (NMJ) is a peripheral, cholinergic synapse, that forms between a motor neuron and a skeletal muscle fiber. It is the best studied of all synapses and continues to provide important insights into general synaptogenesis which can be applied throughout the nervous system. The NMJ is a tripartite synapse consisting of a presynaptic motor nerve terminal, a postsynaptic skeletal muscle fiber and terminal Schwann cells (tSCs), specialized glial cells that cap the junction and play multiple roles in synaptic support (Ogata and Yamasaki, 1988) [Fig1.1].

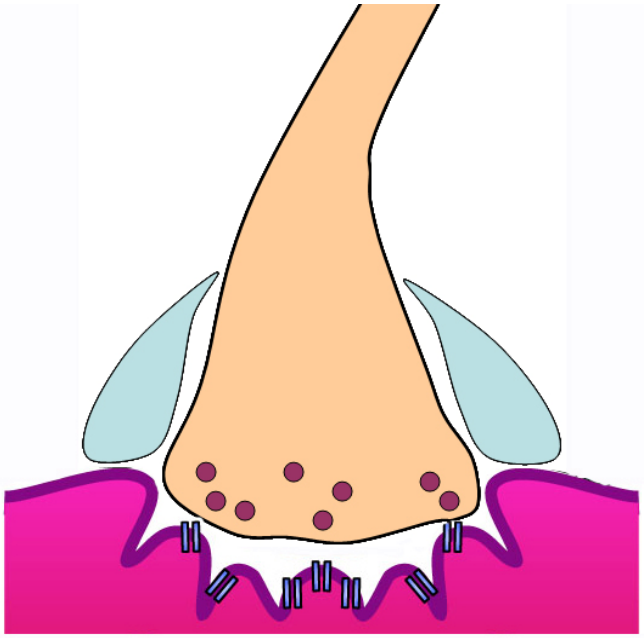

Figure 1.1. Basic structure of the NMJ. Presynaptic motor nerve terminal is shown here with vesicles of neurotransmitter accumulating near the active zone of a nerve terminal. A synaptic space or cleft separates the nerve terminal and postsynaptic muscle fiber (pink). Neurotransmitter receptors are clustered a the top of synaptic ridges in the muscle surface. Terminal Schwann cells cap the synaptic cleft and support the synapse (blue).

Efficient neurotransmission depends on the precise spatial apposition of nerve terminal and neurotransmitter receptors which are found concentrated at the motor endplate (Merlie and Sanes, 1985). One important structural feature of the motor endplate is a high density of acetylcholine receptors (AChRs) which ensures that receptor concentration is not a limiting factor in neurotransmission. These dense receptor clusters are localized near the ridge of specialized grooves in the muscle fiber known as postjunctional folds. AChRs at a mature NMJ are concentrated at levels near 10,000 cm^{-2} (Porter and Barnard, 1975; Fertuck and Salpeter, 1976; Matthews-Bellinger and Salpeter, 1978) and are localized in a complex topographical orientation often described as a "pretzel" shape due to a circular form with fingerlike central projections. [Fig 1.2].

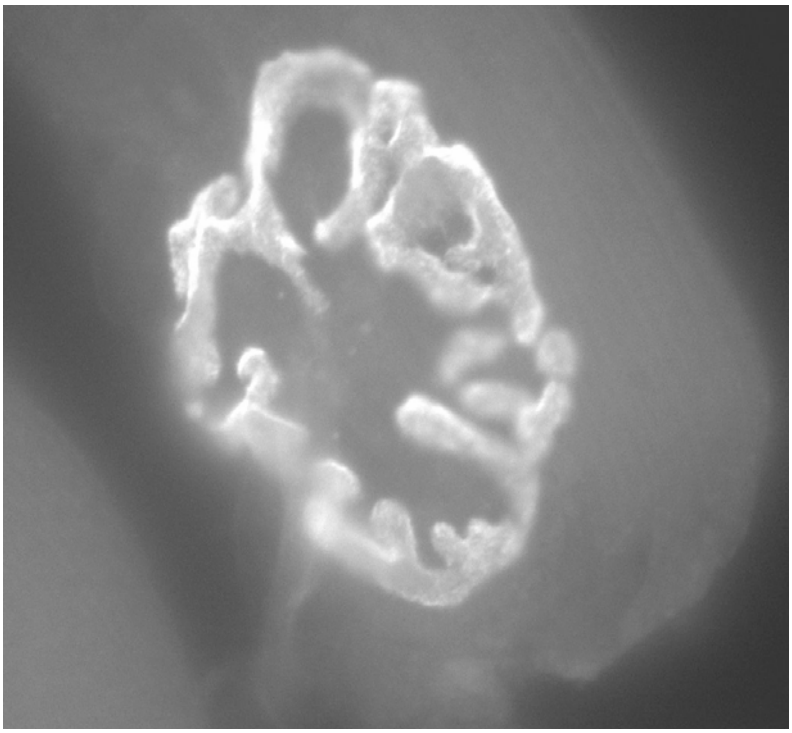

Figure 1.2. Mature AChR cluster. High powered image of a mature pretzel-shaped AChR cluster labeled with fluorescein-conjugated α-bungarotoxin (BXT).

This specialized topography allows the superposition of nerve terminal over regions of high density AChR aggregation. During the process of neurotransmission,

synaptic vesicles, containing the neurotransmitter acetylcholine, accumulate at the active zone and fuse with membrane of the nerve terminal to allow release of acetylcholine (ACh) into the synaptic cleft. This process allows neurotransmitter binding to AChRs on the surface of the postsynaptic muscle fiber. While many aspects of NMJ function and structure have been well characterized, certain processes are less understood, including the mechanisms that initiate formation of these synapses during development and those which determine where a synapse will form.

FORMATION OF THE NMJ

Muscle differentiation and patterning of the postsynaptic specialization

The formation of skeletal muscle is initiated during the process of myogenesis, when multinucleated myofibers or myotubes are formed by the fusion of mononucleated myoblasts (Horsley and Pavlath, 2004). Many in-vivo studies of NMJ formation have utilized the diaphragm muscle due in part to the critical need for muscle contraction during breathing. During development of the mouse diaphragm, primary myofibers are differentiated prior to embryonic day (E) 12–14 at nearly the same time that motor axons are growing ventrally toward the muscle (Witzemann, 2006). Early receptor clusters have been described which correspond to the time of myotube formation. These clusters that are concentrated in the central regions of the myofibers are termed a receptor "pre-pattern" which refers to their appearance in muscle prior to innervation by motor axon (Braithwaite and Harris, 1979; Lupa and Hall, 1989; Lin et al., 2001; Yang et al., 2001). The clustering of AChRs in skeletal muscle depends on complex signaling interactions including signaling involved in the synapse-specific expression of neurotransmitter receptors, and signaling that organizes postsynaptic proteins. Two protein signaling pathways have been well studied as contributors to synapse formation: neuregulin-1

(Nrg-1) activation of the epidermal growth factor receptor (ErbB) tyrosine-kinase receptors (Fischbach and Rosen, 1997), and the activation of muscle-specific tyrosine kinase (MuSK) by neuronal agrin (McMahan, 1990).

Neuregulin/ErbB receptor signaling

Many studies of NMJ formation have focused on understanding the cellular and molecular mechanisms underlying the clustering of AChRs. This is due in part to the fact that AChR clustering is an early event in the formation of synapses. Study of AChRs has also been facilitated by the availability of α-bungarotoxin (BTX), a venomous snake protein that binds almost irreversibly to the AChR and can be chemically conjugated to a number of detectable chemical moities. Concentration of AChRs at the NMJ requires not only the clustering of AChRs, but also local synthesis of AChRs at the synapse. The neuregulins are a group of alternatively-spliced proteins that activate a family of epidermal growth factor receptor (ErbB) tyrosine kinases found in skeletal muscle (Holmes et al., 1992). Nrg-1 was originally isolated from chick brain as a factor able to stimulate AChR synthesis in cultured myotubes. Neuregulin binding induces ErbB receptor dimerization, autophosphorylation, and the eventual activation of acetylcholine receptor gene transcription (Holmes et al., 1992; Corfas et al., 1993; Falls et al., 1993; Sandrock et al., 1997). ErbB receptors are localized to neuromuscular synapses and their concentration has been thought to contribute to synapse-specific transcription of AChR subunits (Altiok et al., 1995; Jo et al., 1995; Moscoso et al., 1995). Although early evidence (Sandrock et al., 1997) suggested that Nrg-1 may be the nerve-derived factor which controls the local synthesis of AChRs, additional evidence has clouded our understanding of the neuregulins roles in synapse formation. In one study, a targeted deletion of one form of membrane-bound neuregulin resulted in peripheral nerves lacking Schwann cells (Wolpowitz et al., 2000) suggesting that the neuregulins play a role in

survival of these cells. A similar result was seen in mice that lacked nrg-1 in motor and sensory neurons (Jaworski and Burden, 2006) and in ErbB2-/- mice with a rescued, selective expression of ErbB2 in heart muscle (Morris et al., 1999; Woldeyesus et al., 1999). While the Schwann cells were affected in these experiments, the levels of AChR transcription were marginally affected which suggests that Nrg-1 expression is not critical for synaptic AChR transcription. More recent loss-of-function studies in mice (Escher et al., 2005; Jaworski and Burden, 2006) have shown that Nrg-1 is not necessary for synaptogenesis, but may only modulate synapse-specific AChR expression. Additional in vivo work supports the notion that neuronal nrg-1 is not critical for postsynaptic organization such as evidence that MuSK activation induces AChR clustering in the absence of innervation (Cohen et al., 1997; Jones et al., 1997; Meier et al., 1997). Additional recent evidence shows that inactivation of nrg-1 in motoneurons, muscle fibers and both cells using Cre/loxP recombination had no effect on AChR clustering, although mice lacking neuronal nrg-1 died at birth due to the absence of Schwann cells (Jaworski and Burden, 2006). Therefore, although evidence supports a role for Nrg signaling in tSC development and survival, evidence has shown that nrg-1 may not have a critical role in synapse-specific AChR transcription.

MuSK and postsynaptic organizers

Refinement of the AChR pre-pattern is thought to require both local molecular signals and communication between nerve and muscle fibers that together result in a mature cluster pattern which is narrower than the pre-pattern. A number of in vitro and in vivo studies have generated evidence supporting the hypothesis that agrin is the essential factor used by motor neurons to induce and/or refine AChR clustering at the NMJ. Agrin was initially isolated from Torpedo electric organ where it was found to induce clustering of AChRs on cultured myotubes (Nitkin et al., 1987). Agrin is

expressed by all three synaptic cell types although studies have shown that agrin is subject to alternative splicing which generates isoforms with varied clustering activities. Agrin isoforms produced by motor neurons have strong clustering activity while those produced by muscle or Schwann cells lack significant aggregating activity (Ruegg et al., 1992). Agrin released at the synapse activates MuSK signaling through a MuSK-associated "myotube-associated specificity complex" (MASC) (Glass et al., 1996). Signaling via MuSK activation is critical to NMJ formation as agrin mutant mice fail to form neuromuscular synapses, are immobile, and die in utero or are stillborn (Gautam et al., 1996). Additionally, MuSK itself was found critical for synaptogenesis as mice that were homozygous for a mutation in the MuSK catalytic domain showed abnormal nerve and AChR patterning (Jennings et al., 1993; Valenzuela et al., 1995; Glass and Yancopoulos, 1997). MuSK mutant mice lack all known features of postsynaptic differentiation, including the concentration of proteins normally localized to NMJs including AChRs, acetylcholinesterase, ErbB3, and ErbB4 (DeChiara et al., 1996; Gautam et al., 1996). MuSK mutant mice also lack an early AChR pre-pattern suggesting that MuSK activity is necessary for establishing early AChR patterning (Lin et al., 2001; Yang et al., 2001). Presynaptic differentiation was also disrupted in MuSK mutant mice with disorganized distribution of nerves and disruptions to the shape of nerve terminals (DeChiara et al., 1996). In addition, MuSK signaling experiments were done which substituted a kinase domain from an alternative tyrosine kinase for the MuSK activation domain. In these experiments, the altered kinase signaling was able to restore most aspects of pre- and postsynaptic differentiation (Herbst et al., 2002). In addition to MuSK, another molecule that plays an important role in agrin signaling is rapsyn. Rapsyn is an intracellular, membrane-associated protein which is found associated stoichiometrically with the AChR. Rapsyn-/- mice were shown to have no AChR

clusters, and studies in rapsyn-/- myotubes showed no AChR clusters following agrin application (Gautam et al., 1995). Other functions have also been attributed to agrin signaling including tyrosine phosphorylation of the β-subunit of the AChR (Wallace, 1991; Ferns et al., 1996). While β-subunit phosphorylation does not seem critical for receptor clustering in muscle cultures (Meyer and Wallace, 1998), it may serve to stabilize the interaction between the AChR clusters and the intracellular cytoskeleton (Borges and Ferns, 2001). The treatment of myotubes with the tyrosine kinase inhibitor staurosporine uncouples agrin-induced MuSK phosphorylation from AChR-β phosphorylation (Fuhrer et al., 1997), which suggests that MuSK is not the kinase that phosphorylates AChR-β in response to agrin. At this time, the best candidates for this function are the Src-family of tyrosine kinases and the Abl kinases. The Src-kinases are associated with AChRs and are activated by agrin (Mittaud et al., 2001), and Abl kinases have been shown necessary for agrin-induced clustering in myotubes (Finn et al., 2003). Although experimental evidence supports a role for these molecules in the agrin-signaling pathway, there are no in-vivo loss-of-function studies for them which have produced a phenotype similar to agrin-, MuSK-, or rapsyn-deficient mice. We must therefore continue to consider them as modulators and not critical components of the agrin-MuSK signaling cascade in muscle. In addition, recent studies have identified two additional candidates which may be critical for postsynaptic organization. Low-density lipoprotein (LDL) receptor-related protein (LRP) family members are known to have specific roles in the development and function of the mammalian nervous system, as receptors for both known and unknown ligands (May and Herz, 2003). Lrp4 null mutants were generated and showed a loss of all signs of postsynaptic specialization, including a loss of MuSK, Rapsyn, utrophin and AChR clustering. Similar to MuSK mutants, AChR clusters were absent at E13.5 and motor axons extended past the normal endplate region

and showed extensive branching across the surface of the muscle. Lrp4 seems to be necessary for all aspects of postsynaptic specialization and may act upstream or with MuSK to establish a NMJ (Weatherbee et al., 2006). Another group searched for factors that can bind MuSK and achieve MuSK activation. Dok-7 was identified based on sequence elements, and Dok-7 null mice showed lethality at birth and an absence of AChR clusters (Okada et al., 2006).

RETHINKING THE CLASSICAL MODEL

The classical view of synapse formation was proposed as a result of early evidence including the induction of AChRs by agrin. This now classical model postulated that axons would make contact with developing muscle fibers at random sites and release agrin which induced acetylcholine receptor (AChR) clustering and other aspects of postsynaptic differentiation. Presynaptic differentiation would follow, driven by retrograde signals from the muscle that transform the axonal growth cone into a nerve terminal. In this model the nerve serves as the inducer of postsynaptic differentiation (McMahan, 1990). During normal neuromuscular junction formation, synapses typically localize to an "endplate zone" in the middle of muscle fibers, which is also the region of initial AChR prepattern. According to the classic view, this location results from the initial contact by the nerve as it grows into the muscle. A number of early studies support this neuronal model. In one study, nerves transplanted onto extrajunctional region of denervated adult rat soleus muscles induced synapses that were similar to NMJs that form during development (Fex and Thesleff, 1967). Other studies showed that co-cultured neurons and muscle in vitro could form synapse (Anderson and Cohen, 1977; Frank and Fischbach, 1979). In these cultures, neurites failed to contact pre-formed, spontaneous AChR clusters, but alternatively induced AChR clusters de novo in other regions of the myotube surface. Simply stated, the nerve-dependent model predicts axons are capable

of inducing synapses anywhere on the muscle fiber. This notion took firm root in the field, and led to a search for possible factors involved in synapse formation. However, more recent results have emerged to challenge the classical paradigm. Some researchers have suggested that the initial nerve-muscle contact is not random but is directed to the middle of the muscle fiber by the pre-pattern of AChR clusters present in the central area of fibers (Yang et al., 2000; Lin et al., 2001; Yang et al., 2001). In this model, NMJs preferentially form in the endplate zone as wandering axons contact pre-formed, nerve-independent AChR clusters in the central region. These early contacts would then form mature synapses by the action of nerve-derived synaptogenic signals such as agrin and acetylcholine. In this model the muscle is the inducer of postsynaptic differentiation (reviewed in (Arber et al., 2002; Kummer et al., 2006). This newly proposed model is supported by early in-vitro evidence from muscle cell cultures showing that AChR clusters formed "spontaneously" on the surface of muscle cells (Vogel et al., 1972; Fischbach and Cohen, 1973). A growing body of evidence has also shown the presence of clusters in the absence of nerve. Two research groups independently generated knockout mice for the transcription factor Hb9 (Arber et al., 1999; Thaler et al., 1999) and showed that nerve-independent, muscle-dependent AChR clusters were present in the central region of Hb9-/- diaphragm muscle (Lin et al., 2001; Yang et al., 2001). In an early study, Braithwaite and Harris caused pharmacological damage to motor axons in rat embryos and still observed AChR clusters which accumulated as a central band in muscles (Braithwaite and Harris, 1979). In addition, Dahm and Landmesser noted that AChR clusters appeared in chick embryo muscle just before the nerve entered the muscle (Dahm and Landmesser, 1991). Sohal reported AChR clusters in avian embryos which lacked motor neurons (Sohal, 1988). All of these findings taken together, support the notion that muscle could indeed induce AChR clustering. With advances in genomics

and especially the sequencing of whole genomes, additional models systems are rising in popularity. The optical transparency of zebrafish embryos has made them a wonderful model for investigating synptogenesis while vitally imaging synapse formation during embryogenesis. Results from in-vivo imaging of developing neuromuscular junctions showed that extending axon appeared to make contact with pre-existing AChR clusters. This result suggests that early AChR clusters may be the site of synapse formation (Panzer et al., 2006), although not exclusively (Flanagan-Steet et al., 2005). However, zebrafish and mammalian neuromuscular synaptogenesis differ in several important aspects (Panzer et al., 2005), which leaves some question as to whether these results will also apply to mammals. The muscle-dependent (prepattern) model would predict that muscle can control the site of synapse formation by providing an early marker for initial axonal contact.

RATIONALE FOR THIS STUDY

Our laboratory recently published results (Ponomareva et al., 2006) which showed that tetracycline-controlled, muscle-specific expression of a constitutively active ErbB2 (CAErbB2) receptor during embryogenesis produces a phenotype in which AChR clusters disperse by embryonic day (E) 15.5, axons sprout along muscle fibers and synapses fail to form leading to embryonic lethality. Two features of this phenotype were useful for purposes of this study: that clusters forming prior to E15.5 (pre-pattern of AChRs) would be dispersed, and that axons extended throughout diaphragm muscle would be forced into regions of diaphragm where early pre-pattern of clusters would not have formed. Since our genetic system allows us to control the timing of CAErbB2 expression in these mice, we were able to investigate whether and where synapses would form by birth after withdrawal of the antibiotic inducer. We wondered whether synapses would form, and whether or not synaptic function could be restored. My work will be

presented as follows: Chapter two contains the manuscript in which I present the major body of work done for this dissertation. This manuscript has been submitted for publication. In chapter three I present additional data and results related to this project. In chapter four I will summarize my findings and discuss the greater implications of my work. Finally, in chapter five I will provide detailed methods for my work.

CHAPTER 2

Evidence for muscle-dependent neuromuscular synaptic site determination in mammals

INTRODUCTION

The vertebrate neuromuscular junction (NMJ), the synapse between a motor neuron and a skeletal muscle fiber, is the best studied of all synapses and it continues to provide important insights into general synaptogenesis throughout the nervous system. In the now classic paradigm, axons contact developing muscle fibers at random sites and release agrin, a proteoglycan which induces acetylcholine receptor (AChR) clustering, and other aspects of postsynaptic differentiation, upon activation of a muscle membrane receptor complex containing the receptor tyrosine kinase MuSK. Presynaptic differentiation follows driven by retrograde signals from the muscle that transform the axonal growth cone into a nerve terminal. In this model the nerve is the inducer of postsynaptic differentiation (McMahan, 1990). Neuromuscular junctions localize to an "endplate zone" in the middle of muscle fibers. According to the classic view, this location results from the initial contact by the nerve of short embryonic myotubes that later grow by fusion of more cells at their ends. Recently, however, this view has been challenged by evidence suggesting that the initial nerve-muscle contact is not random but is directed to the middle of the muscle fiber by a pre-pattern of AChR expression and clustering present in the central area of the fibers (Yang et al., 2000; Lin et al., 2001; Yang et al., 2001; Lin et al., 2005; Misgeld et al., 2005). Thus, NMJs localize to the endplate zone from the beginning of synaptogenesis as wandering axons preferentially contact pre-formed, nerve-independent AChR clusters in the central area. These sites mature into synapses by the action of nerve-derived synaptogenic signals such as agrin

and acetylcholine. In this model the muscle is the inducer of postsynaptic differentiation (reviewed in (Arber et al., 2002; Kummer et al., 2006).

The optical transparency of zebrafish embryos has made possible the testing of these models by vitally imaging whether the aneural AChR clusters are incorporated into nascent synapses. Results from these experiments suggest that these clusters are commonly (Panzer et al., 2006), but not exclusively (Flanagan-Steet et al., 2005), the site of synapse formation. However, zebrafish and mammalian neuromuscular synaptogenesis differ in several important aspects (Panzer et al., 2005), thus, it remains open whether these results also apply to mammals. Live imaging of early mammalian synaptogenesis is currently unfeasible, nevertheless, another approach to examine the role of the prepattern is to probe whether embryonic axons can induce synapses de novo if they are driven to grow outside the central area of the muscle where the pre-pattern localize. In their simplest forms, the nerve-dependent model predicts axons will induce synapses anywhere on the muscle fiber if given the chance, whereas the muscle-dependent (i.e. prepattern) model predicts they will not.

We recently showed (Ponomareva et al., 2006) that tetracycline-controlled, muscle-specific expression of a constitutively active ErbB2 (CAErbB2) receptor during embryogenesis produces a phenotype in which AChR clusters disperse by embryonic day (E) 15.5, axons sprout along muscle fibers without stop and synapses fail to form leading to lethality at birth. As we also control the timing of CAErbB2 expression in these mice, here we asked whether and where synapses would form by birth after withdrawal of the antibiotic inducer. We find that axons continue to sprout following doxycycline (Dox) removal at E15.5 and stop seemingly at random to engage in synaptogenesis all along the entire width of the diaphragm muscle. Although, at first glance, this finding is consistent with the nerve-dependent model, we find that the same widely diffused pattern of AChR

clusters is generated in diaphragms with similar transient expression of CAErbB2, but that lack altogether the phrenic nerve by genetic ablation of the Hb9 gene (Arber et al., 1999; Thaler et al., 1999). Thus, as previously shown for the central AChR cluster pre-pattern, the random pattern of AChR clusters generated in our experimental paradigm is nerve-independent. These results support a role for the muscle fiber in determining the site of initiation in mammalian neuromuscular synaptogenesis in vivo.

MATERIALS AND METHODS

Mice

The transgenic lines harboring cDNAs encoding a reverse tetracycline transactivator (rtTA) or a constitutively active ErbB2 receptor (CAErbrB2) were previously described (Ponomareva et al., 2006). Homozygous CAErbB2 males were crossed to heterozygous rtTA females. Both, single transgenic (ST, rtTA-/-; CAErbB2+/-) and bi-transgenic (BT, rtTA+/-; CAErbB2+/-) embryos were generated from the same cross. The former (ST) served as control whereas the latter (BT) were the experimental animals. Heterozygous HB9 mice (kindly provided by S. Burden, New York University, with permission from T. Jessell, Columbia University, NY) were crossed into BT animals to generate BT progeny that was also HB9 null (BT Hb9-/-) and lacked phrenic innervation of diaphragm as previously described (Arber et al., 1999). A transgenic line expressing green fluorescence protein (GFP) under the control of S100 regulatory sequences (kindly provided by W. Thompson, University of Texas at Austin, TX, (Zuo et al., 2004)), was crossed with the rtTA mice in order to produce females who were GFP+/-; rtTA+/-. Crossing these females with homozygous CAErbB2 males produced ST and BT progeny that had GFP-labeled Schwann cells.

Mouse genotyping

Genomic DNA was prepared following standard methods. Genotyping was done by PCR using FastStart Taq DNA polymerase (Roche,). Primers were as follows: (i) rtTA: Forward, 5'-AGAGCACAGCGGAATGACTT-3'. Reverse: 5'-GCCTGACGACAAGGAAACTC-3'. (ii) CAErbB2:IRES:Luciferase: Forward: 5'-CTTCTTCGCCAAAAGCACTC-3'. Reverse: 5'-CACACAGTTCGCCTCTTTGA-3'. (iii) HB9 deletion: Forward: 5'-TGCACAGGCGGCTCTCTATGG- 3'. Reverse: 5'-CCACAGCTCGCTAGGAGGTGAG-3'. (iv) GFP: Forward: 5'-AATCGAGTTGAAGGGCATTG-3'. Reverse: 5'-GCCGATTGGAGTGTTCTGTT-3'

Doxycycline induction

Doxycycline (Dox, Sigma, St. Louis, MO) was mixed with customary ground mouse food, sucrose, and water. For 1g of food, we added 6 mg Dox, 5% sucrose, and water to make a paste that was cut into pellets. Dox-containing food was given to pregnant dams at the time indicated in the text. Dox reached the embryos through the placenta. All animal experimentation was approved by the University of Texas Institutional Animal Care and Use Committee.

Luciferase assay

Muscles were homogenized in Luciferase Cell Culture Lysis Reagent (Promega, Madison, WI) and centrifuged at 4°C. Twenty microliters of cleared lysate was added to a Chromalux flat bottom plate (Dynex). Luciferase activity assay was performed on a Dyanex MLX Microplate Luminometer using 40 µl Luciferase Assay Reagent (Promega, Madison, WI) with a total read time of 10s. Total light units obtained from reading were normalized to total protein content determined by Bradford assay (Biorad, Hercules, CA).

Immunohistochemisty

Diaphragm muscles were immunostained as previously described (Ponomareva et al., 2006). Embryonic day (E) 14 and E15 whole embryos were removed and fixed in 4% paraformaldehyde (PFA) at 4◦C overnight. The next day, concentrated PFA was replaced with 0.4% PFA until diaphragm dissection (1-4 days following embryo removal). Older (E16, E17, E18) embryos and neonates were fixed in 2% PFA and replaced with 0.2% PFA as described above. Diaphragms were dissected and washed 2 times in PBS for 5 minutes each in multi-well culture dish. Axons and nerve terminals were labeled with polyclonal rabbit anti-neurofilament at 1/500 (Chemicon, now Milipore , Billerica, MA) and anti-synaptophysin at 1/200 (Zymed, now Invitrogen, Carlsbad, CA). Rhodamine-conjugated, anti-rabbit IgG secondary (Jackson Immunoresearch, West Grove, PA) was used to visualize neuronal markers, while acetylcholine receptors (AChRs) were labeled with fluorescein-α-bungarotoxin (BTX, Molecular Probes, Eugene, OR) at 1/1000. Samples were mounted in Vectashield (Vector Labs, Burlingame, CA) and viewed in a Eclipse E-1000 fluorescence microscope (Nikon) equipped with filters selective for either fluorescein or rhodamine.

In situ hybridization

Diaphragms from E15.5 embryos and postnatal day (P) 0 were dissected and fixed overnight in 4% PFA in PBS. A previously described probe for AChRα (Rimer et al., 2004) (Rimer et al., 2004) and a 1317 bp-probe for mouse AChRε cDNA (AChRε ISH2, kindly provided by S. Burden, New York University, NY) were labeled with digoxigenin, chemically hydrolyzed (Schaeren-Wiemers and Gerfin-Moser, 1993), and used for whole-mount in situ hybridization following a protocol originally described for tissue sections (Braissant and Wahli, 1998).

Confocal microscopy

High resolution, high magnification images were captured using a Leica SP2 AOBS Laser Scanning Spectral Confocal Microscope (Leica Microsystems). A 63X oil (HCX PL APO 1.4-.60 NA Blau CS) objective with digital zoom allowed captured images at approximately 120X magnification.

Regions of diaphragm muscle containing groupings of several synapses were first localized using a low power objective lens. High-power images were obtained where at least one cluster was visible "en face", oriented toward the viewer. Z stacks were 0.12 um thick. To measure postsynaptic area, stacks were rotated using the Metamorph software tool (Molecular Devices Corporation, Downingtown, PA) until one cluster of the region was visible en face. A maximal projection was generated from the stack and the border around the en face AChR cluster was thresholded. This was repeated for six en face clusters from each ST and BT animal. Area occupied by labeled AChRs was measured and Students' t-test was done to determine whether cluster area differed between control and experimental animals.

Aneural AChR cluster analysis

Diaphragm muscle from E16.5, E17.5 and P0 was visually scanned using the 40x objective (NA 1.30, Nikon) in the widefield microscope described above . Three to five regions of lateral, normally extrajunctional zone were examined in BT samples, while 1-2 regions adjacent to the center of the muscle were examined in ST samples. In all cases, regions selected were either dorsal or ventral to region of phrenic nerve branching. Clusters in a given field were counted, and categorized as either nerve-associated (co-localized with nerve terminal staining) or aneural (not near a visible nerve terminal). Planes above and below the plane of focus for the AChR clusters were scanned to confirm the absence of nearby axonal processes.

Synapse / aneural AChR cluster pattern distribution analysis

Montages were created by aligning adjacent images of diaphragm muscle taken with the 10X objective (NA 0.30, Nikon) of the widefield microscope. All images were obtained from the region of diaphragm just ventral to the area where phrenic nerve branching occurs. The width of hemi-diaphragm was then determined by drawing a line across the width of the assembled collage. The mid line of hemi-diaphragm width was marked on each collage along with a short line, perpendicular to width line and extending above the width line for a distance of 1/30th of muscle width. The distance between random AChR clusters and the midline was measured and recorded. Sixty cluster distances were obtained from hemi-diaphragms of 3 embryos for each genotype. Analysis of variance was calculated using distance measurements normalized to the total measured width of hemi-diaphragm from each animal.

RESULTS

Removal of AChR clusters by E15.5

Our laboratory previously showed that in-vivo induction of a ligand-independent, constitutively active form of the ErbB2 receptor (CAErbB2) throughout murine embryogenesis resulted in the disappearance of AChR clusters from skeletal muscle (Ponomareva et al., 2006). To determine the extent of AChR cluster loss following a limited induction of the CAErB2 receptor, we used the previously described tet-on genetic system, that employs a CAErbB2 sequence downstream of a tetracycline inducible sequence. Heterozygous females for a muscle-specific reverse-tetracycline trans-activating protein (rtTA+/-) were crossed with males homozygous for the CAErbB2 receptor (CAErbB2+/+) in order to produce experimental and control animals in each litter. Following verification of conception, expectant females were given doxycycline-

containing rodent food for a limited period during gestation, beginning induction on E11.5 and continuing until E15.5 when Dox was removed from food. Litters were taken at E15.5 and whole-mount diaphragm immunostaining was performed to determine the extent of receptor cluster loss using epifluorescence microscopy. Axons and nerve terminals were visualized by using antibodies to neurofilament (NF) and synpatophysin (syn), while AChRs were labeled using fluorophore-conjugated α-bungarotoxin (BTX). During normal murine development, the phrenic nerve descends to the rostral side of diaphragm muscle where thick fiber bundles extend and distribute throughout fibers. The bundles branch from a medial position to reach a central region of muscle fiber length, and then extend in both ventral and dorsal directions, running perpendicular to the length of the myofibers. In single transgenic animals, (ST, rtTA-/-; CAErbB2+/-) AChR clusters were found co-localized with nerve terminals near a central region of muscle and proximal to the central nerve bundle (Fig 2.1A,B). Following four days of CAErbB2 expression, however, diaphragm staining from bi-transgenic animals, (BT, rtTA+/-; CAErbB2+/-), showed a complete elimination of AChR clusters from the surface of the muscle (Fig 2.1 C,D). Thus, whether started at conception (i.e. E0.5) as in Ponomareva et al., 2006, or at mid-gestation as done here, induction of CAErbB2 leads to AChR cluster loss by E15.5 in diaphragm muscle.

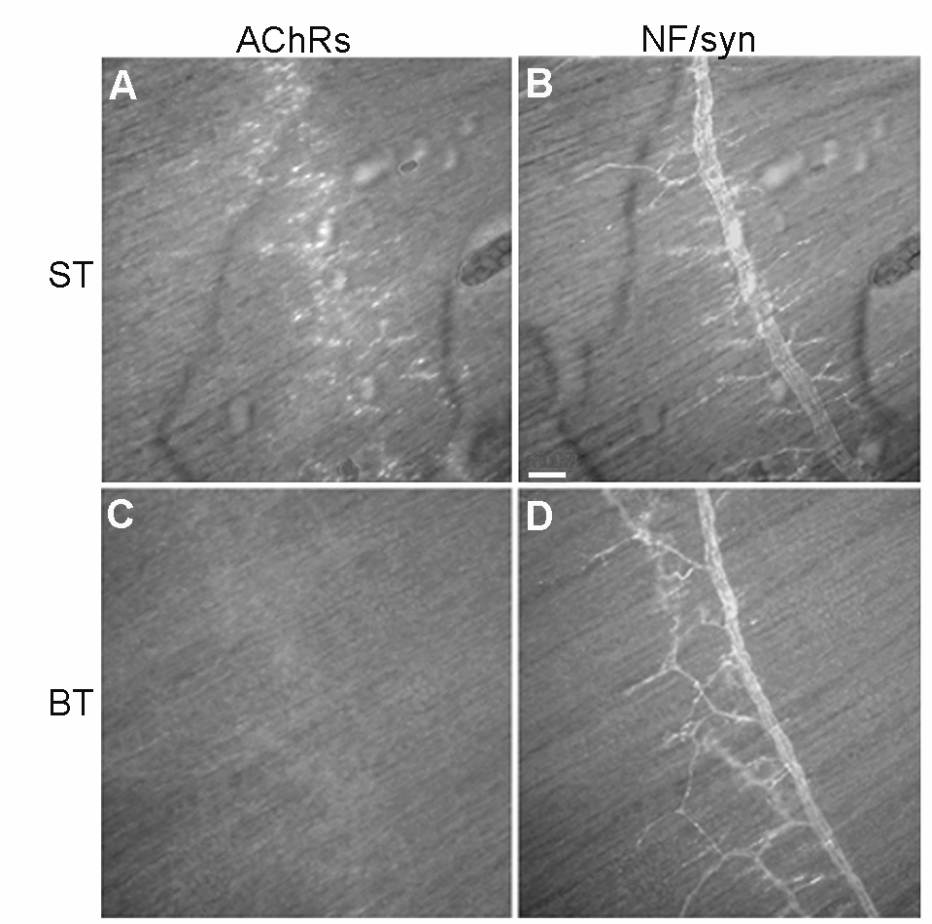

Figure 2.1. Disappearance of AChR clusters following transient CAErbB2 induction. Pregnant rtTA-/- females, fertilized by CAErbB2+/+ males, were fed Dox-containing rodent food from E11.5 to E15.5. Whole mounts of diaphragm muscle from E15.5 ST (A and B) or BT (C and D) embryos were stained with Rhodamine-α-BTX and rabbit anti-NF and anti-syn antibodies. ST diaphragm shows a central location of both AChRs (A) and axons and nerve terminal (B), while BT diaphragm shows the absence of AChR clusters (C) in the area where axons and nerve terminal are labeled. Scale bar: 50μm.

Synapses form by birth throughout the entire width of diaphragm following inducer withdrawal

We had previously determined that in addition to receptor loss, another consequence of CAErbB2 activation throughout gestation was extensive axonal outgrowth. Animals which had induced CAErbB2 signaling throughout gestation

showed axons that extended from the central region of the diaphragm muscle to reach the distal regions of muscle fibers at E18.5 (Ponomareva et al., 2006). As a result of both AChR cluster elimination and nerve outgrowth, synapses failed to form in muscles expressing CAErbB2 (Ponomareva et al., 2006). We sought to restore synapse formation by withdrawing Dox-containing food at E15.5 and allowing elimination of CAErbB2 signaling for a period prior to birth. We reasoned that because of the axonal outgrowth synapses would have to form outside the central region of the muscle, in the absence of a pre-existing AChR pre-pattern. Hence, this manipulation would allow us to test the two models of synapse initiation. The nerve-dependent model would predict that the nerve would be able to induce synapses anywhere along the surface of the muscle fiber, whereas the muscle-dependent model would predict that synapses would form only at sites where there is a pre-existent aneural AChR cluster. Bi-transgenic embryos fed Dox throughout development (or starting at mid-gestation, data not shown) are stillborn as NMJs fail to form by birth. Hence, we anticipated that if synapses were to form after Dox withdrawal but before delivery, BT pups would be able to survive at birth. Figure 2.2A shows that CAErbB2+/-; rtTA+/- mice were indeed recovered among surviving pups at P0 in litters where Dox was withdrawn at E15.5. Their frequency was consistent with a Mendelian distribution. As expected, the survival of BT animals correlated with a drop in transgenic expression. Figure 2.2B shows that there was a 100-fold decrease in transgene expression in BT embryos at E17.5 after Dox withdrawal at E15.5.

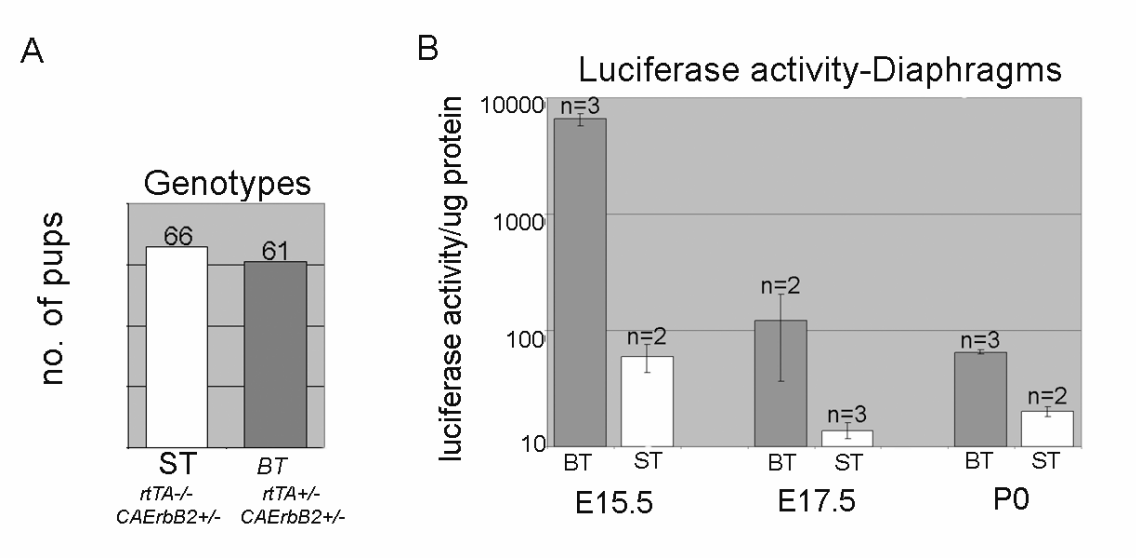

Figure 2.2. Survival at birth and reduction in transgene expression after Dox withdrawal. (A) Genotyping results from 14 experimental litters (127 animals total). Crosses were: rtTA+/- female X CAErbB2+/+ male. Tail snips were taken after pups were born at P0. The even number of ST (rtTA-/-; CAErbB2+/-) and BT (rtTA+/-; CAErbB2+/-) pups reflects expected Mendelian genetic frequency if all BT animals survive at birth. (B) The CAErbB2 transgene has an internal ribosomal entry sequence and a firefly luciferase ORF cloned in-frame downstream. So, from one mRNA, two proteins, CAErbB2 and luciferase, are translated. Hence, luciferase activity is used as surrogate for CAErbB2 expression. Diaphragm muscle extracts were used to measure luciferase activity. At E15.5 when Dox-food was removed, average luciferase activity is high in extracts from BT diaphragm. By E17.5, average luciferase activity is reduced nearly 100-fold. By birth average luciferase activity is reduced to levels in ST controls. Results are presented as mean ± standard error.

We performed immunostaining of whole-mount diaphragms from P0 pups to determine the location of synapses. Diaphragm muscle from survival animals was labeled for presynaptic and postsynaptic markers as above. Single-transgenic, control animals showed the expected central co-localization of nerve and receptor clusters (Fig 2.3). On the other hand, muscle staining from recovered BT neonates showed that synapses were not exclusively localized in the central zone of the muscle, but that nerves had extended and grown out throughout the diaphragm as previously observed with CAErbB2

induction throughout gestation. Some nerve terminals and AChR clusters were seen co-localized even near the edges of diaphragm muscle (Fig 2.3).

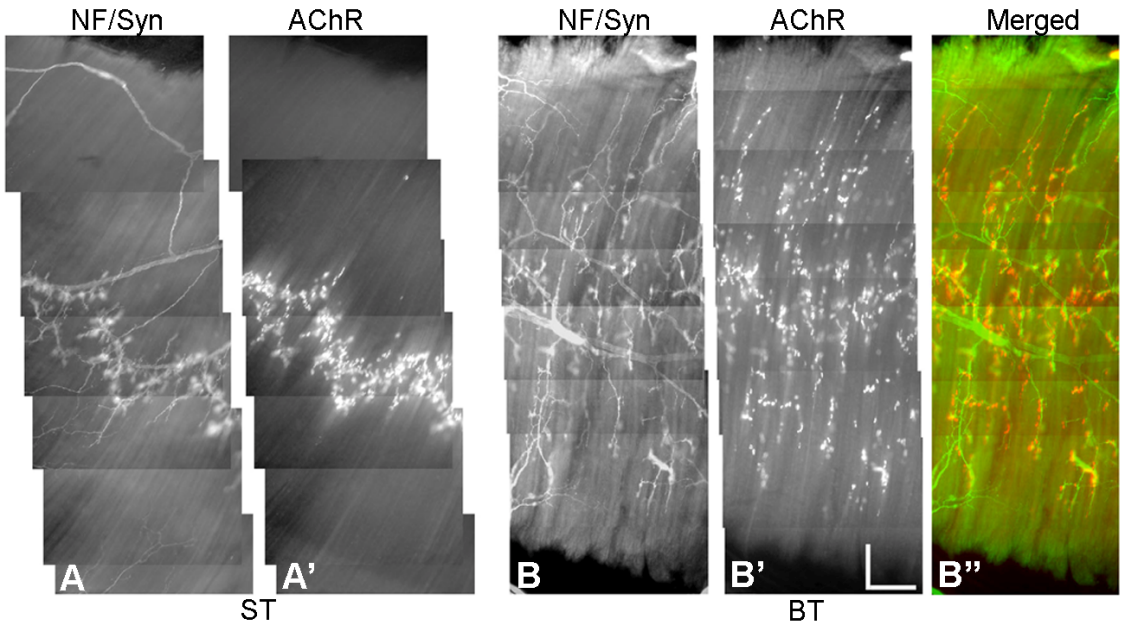

Figure 2.3. Widely distributed pattern of innervation in BT animals after transient CAErbB2 induction. Whole mounts of diaphragm muscle from P0 BT and ST animals were stained for AChRs and axons/nerve terminals as in Fig 2.1. Images were aligned in a montage to show the pattern of innervation from one side of diaphragm to the other. (A and A') ST muscle shows central, focal patterning of both nerve and nerve terminal (A) with co-localized AChR clusters (A'). (B – B") BT animals showed extensive nerve outgrowth (B) and AChR clusters that were distributed throughout the width of diaphragm (B'). A color overlay shows the co-localization of nerve terminal and receptor clusters (B"). Scale bars: 200 μm.

High-power, confocal views of these synapses showed normal apposition between nerve terminals and AChRs (Fig 2.4). No aneural AChR clusters were observed at P0 (see also Fig 2.6B, below). Further characterization of the restored synapses in BT muscle at P0 showed that the area covered by the AChRs was similar to control synapses (n= 6 for each ST and BT. $P=0.9051$, $P<0.05$; Student's T-test). In addition, terminal Schwann cells as well as acetylcholinesterase were present in BT synapses (Figure 3.3, 3.4). Thus,

synapses are restored in BT diaphragm by birth after withdrawal of Dox. They appear similar to control synapses except that they localize over the entire surface of the muscle.

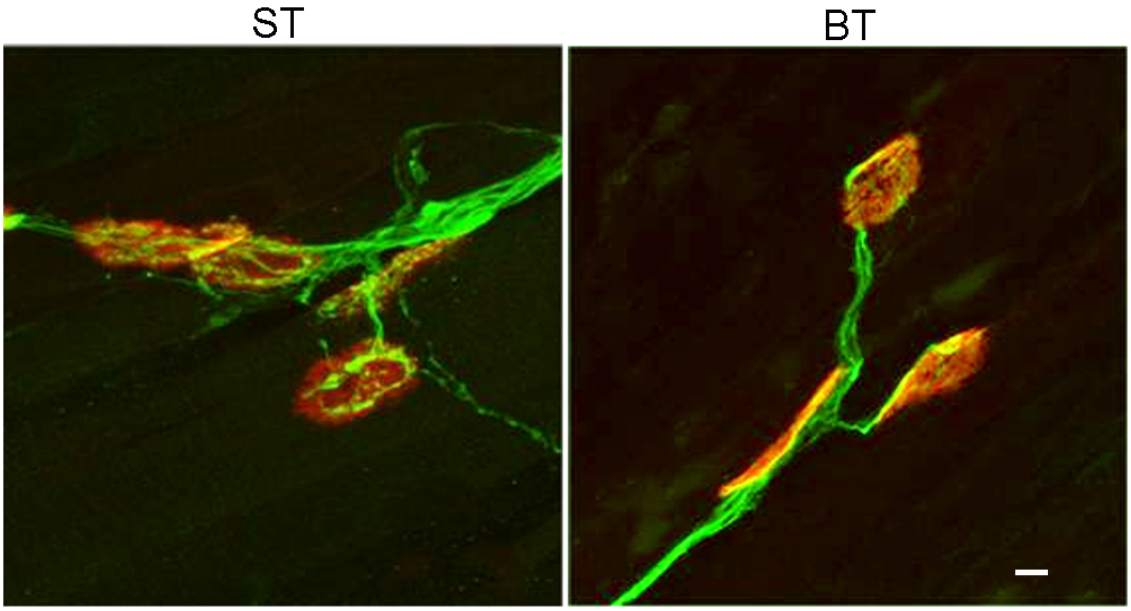

Figure 2.4. Proper pre- and postsynaptic apposition in restored synapses after transient CAErbB2 induction. Representative high-power, maximal confocal projections of synapses in ST and BT P0 diaphragms after transient embryonic CAErbB2 induction. Axon/nerve terminal markers in green, AChRs in red. No aneural AChR cluster were observed at this time. Images such as these were used to estimate AChR cluster area (see text). Scale bar: 5 μm.

AChR transcription reflects spatial distribution of restored synapses

We next checked the distribution of AChR transcripts in our animals. In-situ labeling of AChRα mRNA was done following activation of CAErbB2 until E15.5. The AChRα mRNA in ST animals was highly concentrated in the central zone of muscle fibers as expected (Fig 2.5A). On the other hand, high levels of AChRα mRNA were detected throughout the entire length of the muscle fibers in BT diaphragms at E15.5 (Fig 2.5B). These results are consistent with our previous analysis of AChRα mRNA in E.18.5 BT embryos and with the observed 3-fold increase in AChRα protein levels in the

same muscles (Ponomareva et al., 2006). High levels of transcript could result from the combination of synaptic contact loss (i.e. denervation) and the activity of CAErbB2 in directly stimulating AChRα transcription throughout the muscle fiber. We also performed in-situ hybridization for AChRα and AChRε mRNAs at P0 in animals which were given Dox-containing rodent food from E11.5 until E15.5. While control littermates showed the expected central localization of receptor transcript (Fig 2.5C,E), labeling for AChRα and AChRε mRNA in experimental animals showed that there were discreet focal accumulations of them throughout the muscle, that were present in a pattern resembling the distributed AChR cluster staining seen before (Fig 2.5D,F). The signal for AChRε transcript was rather weak here, both in ST and BT muscle, because its normal peak of expression occurs at around P7. Thus, following the removal of Dox, AChR mRNA localization changes from a diffused to a focal distribution in BT muscle. This change reflects the process of synapse formation and maturation that occurs after Dox withdrawal. The presence of AChRε mRNA in the restored synapses, that is normally seen only after nerve contact, further confirms the presence of the nerve at these sites.

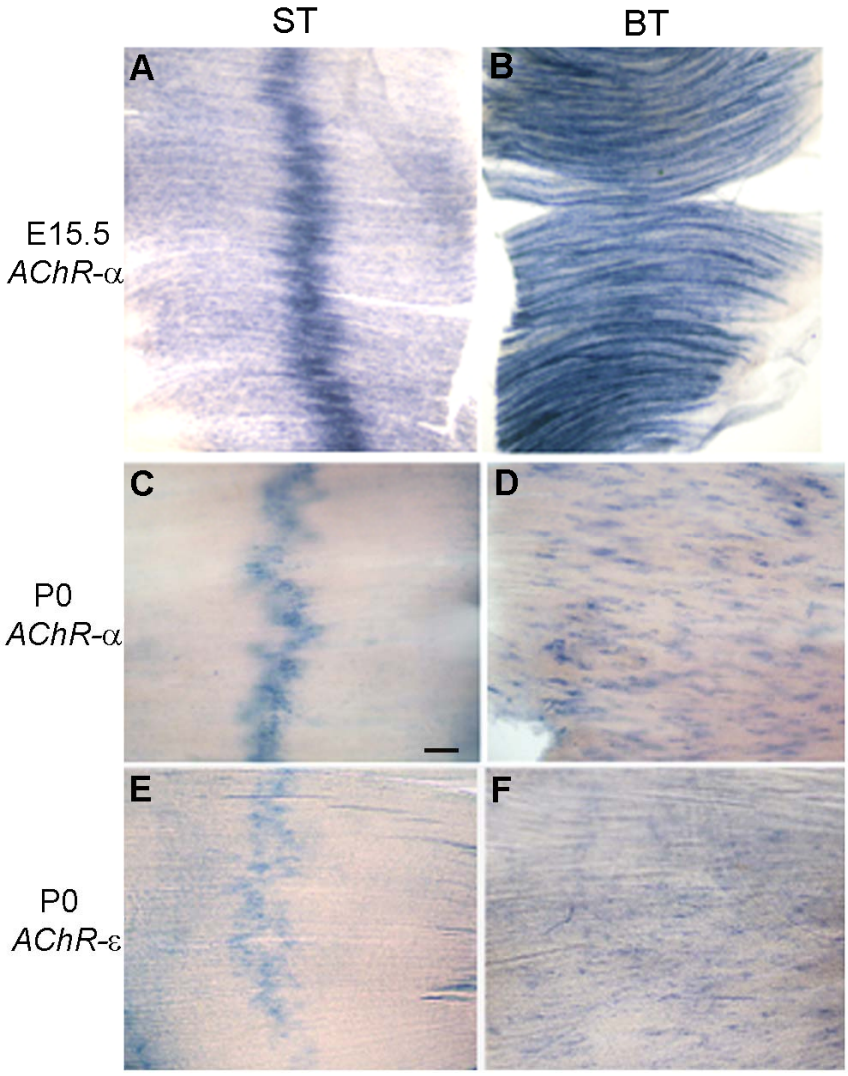

Figure 2.5. Changes in pattern of AChR transcription after transient CAErbB2 induction. (A) Non-radioactive whole-mount in situ hybridization for AChRα mRNA in a control ST E15.5 diaphragm shows transcript concentration in a narrow band in the middle of the muscle. (B) In BT diaphragm, high levels of expression occur throughout the length of muscle fibers. (C) P0 diaphragms from ST animals were labeled for AChRα mRNA and shows a tight band and central localization for AChRα transcription. (D) In BT animals labeled for AChRα mRNA, the distinct focal concentrations of transcription occur throughout the width of diaphragm that appear to mirror the distribution of synapses revealed by protein staining (Fig 3). (E) AChRε mRNA, which is only found localized at synaptic sites, was labeled. In ST animals, it is present in a centrally concentrated pattern. (F) In BT animals, AChRε mRNA appears distributed throughout the diaphragm in distinct focal concentrations. Scale bar: 100μm.

Aneural AChR clusters are observed shortly after Dox withdrawal

So far, the results seem to support the nerve-dependent model as synapses appeared to form without pre-existing AChR clustering or a customary pattern of AChR transcription. This is evident as AChR clusters were absent at the time of Dox withdrawal (Fig 2.1) and there were high-levels of AChR transcript throughout the entire muscle at E.15.5 (Fig 2.5). Nevertheless, because we cannot observe individual synaptic sites over time, we could not rule at this time that aneural AChR clusters formed after Dox withdrawal, and that these would serve as initiation sites for synaptogenesis. To address this possibility, we first examined whether there were aneural AChR clusters ahead of extending nerves during the period of recovery. While immunostaining of recovery animals showed that all distributed AChR clusters at P0 co-localized with nerve, we stained muscle from E16.5 and E17.5 embryos to look for clusters ahead of extending axons. Clusters were examined in 3-5 fields of diaphragm muscle (see Methods), and any clusters that were not co-localized with nerve (described here as "aneural") were tallied (an example in Fig 2.6A). In ST diaphragm only about 2% of clusters were aneural at E.16.5, while about 33% of AChR clusters in BT diaphragm were aneural (Fig 2.6B). In BT diaphragm, only 10% of clusters were found to be aneural at E17.5. By birth no aneural AChR clusters were observed and all clusters were co-localized with a nerve terminal in both ST and BT muscle (Fig 2.6B). Thus, a significant fraction of aneural AChR clusters were found shortly after Dox withdrawal. Their numbers rapidly decline, suggesting that processes leading to synapse formation and maturation are operational during this time.

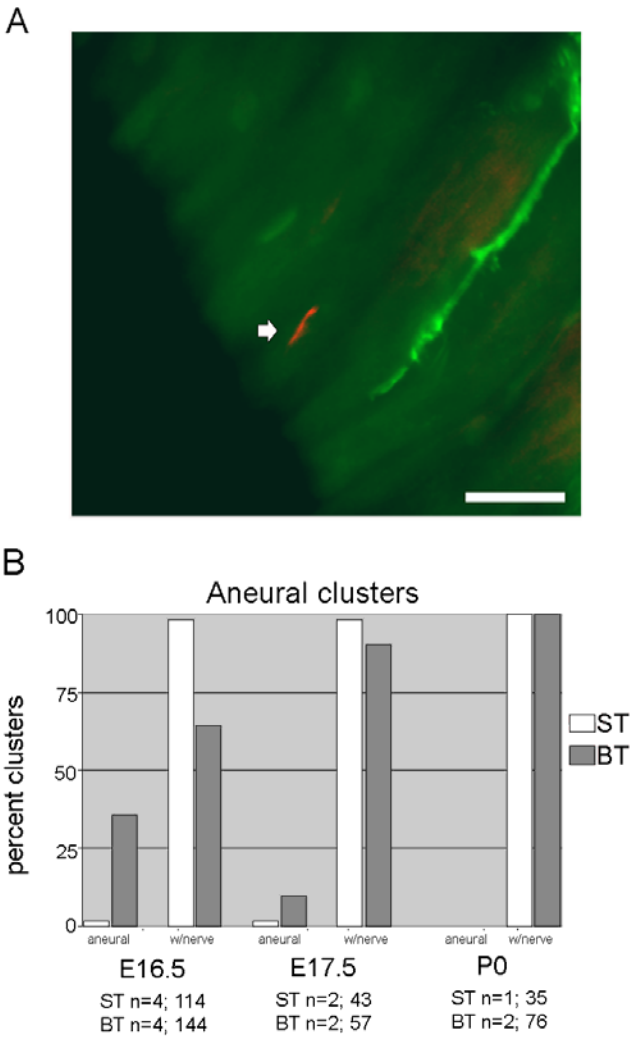

Figure 2.6. Aneural AChR clusters are detected early after Dox withdrawal but disappear by birth. Diaphragm muscle from E16.5 and E17.5 embryos, and P0 neonates was labeled for axons, nerve terminals and AChRs as above. (A) An example of a aneural AChR cluster (arrow) seen near the edge of a E16.5 diaphragm muscle. Scale bar = 25μm. (B) Histogram showing the percentage of clusters counted that were colocalized with nerve terminal and the percent which were deemed "aneural" or where no nerve staining was detected near the site of AChR cluster. At E16.5, ST embryos had 2% aneural clusters, while in BT embryos about 1/3 of total clusters counted were aneural. At E17.5, ST embryos showed nearly no aneural clusters, while in BT animals about 1/10 of total clusters were aneural. By birth however, in both ST and BT animals, no aneural clusters were detected; n= number of diaphragms, total number of clusters.

Nerve is not necessary to generate diffused pattern of AChR clusters

The mere presence of aneural AChR clusters does not rule out the possibility that synaptogenesis after Dox withdrawal in BT mice is induced by the nerve. For example, some of these aneural AChR clusters could result from the release of agrin from growth cones. To test for the necessity of the nerve to induce the spatial pattern of synapses observed in BT diaphragm after removal of Dox, we introduced into our BT animals a mutation in the HB9 transcription factor by crossing with Hb9+/- mice. HB9 null animals lack innervation in diaphragm muscles due to phrenic nerve mis-routing (Arber et al., 1999; Thaler et al., 1999; Yang et al., 2001). We thus generated rtTA+/-; CAErbB2+/-; Hb9-/- (BT Hb9-/-) embryos, and used as controls rtTA+/-; CAErbB2+/-; Hb9+/- (BT Hb9+/-) or rtTA-/-; CAErbB2+/-; Hb9+/- (ST Hb9+/-) litter mates. We fed Dox-containing food to pregnant dams from E11.5 until E15.5. Whole-mount immunostaining of embryonic diaphragm muscle was done to determine whether receptor clusters were present in E15.5 and E18.5 tissue and if found, where they would localize. As observed in BT mice (Fig 2.1), no AChR clusters were detected at E15.5 in BT Hb9-/- mice. Figure 2.7 shows collages of entire sections of diaphragms from embryos of different genotypes at E18.5. As observed at P0, BT Hb9+/- diaphragm at E18.5 showed a diffused pattern of synapses across the entire muscle, while ST Hb9+/- controls showed the typical concentration of synapses in the center on the muscle (Fig 2.7A-B'). Diaphragms from BT Hb9-/- embryos, that lacked phrenic nerve (Fig 2.7C'), showed a distribution of aneural AChR clusters (Fig 2.7C) very similar to the diffused distribution of synapses in BT Hb9+/- diaphragms, that were innervated by phrenic nerve. The distribution of aneural AChR clusters in BT Hb9-/- diaphragms from animals that were given Dox from E11.5 to E15.5 (Fig 2.7C) was also very different (i.e. much wider) from the distribution of aneural clusters in BT Hb9-/- diaphragms from embryos that were

never fed Dox-containing food (Fig 2.7D). Thus, the absence of the phrenic nerve does not seem to impact the distribution of AChR clusters in BT diaphragm, while the absence of muscle expression of CAErbB2 has a great impact on cluster distribution. We tried to quantitatively compare the different distributions by measuring the relative distance from an arithmetic center of random AChR clusters in hemidiaphragm for each experimental genotype (for details see Methods). Figure 2.7F shows that there was no statistical difference between the distributions of AChR clusters between BT Hb9+/- and BT Hb9-/- diaphragms ($F=1.28$, $P<0.005$, One-way ANOVA).

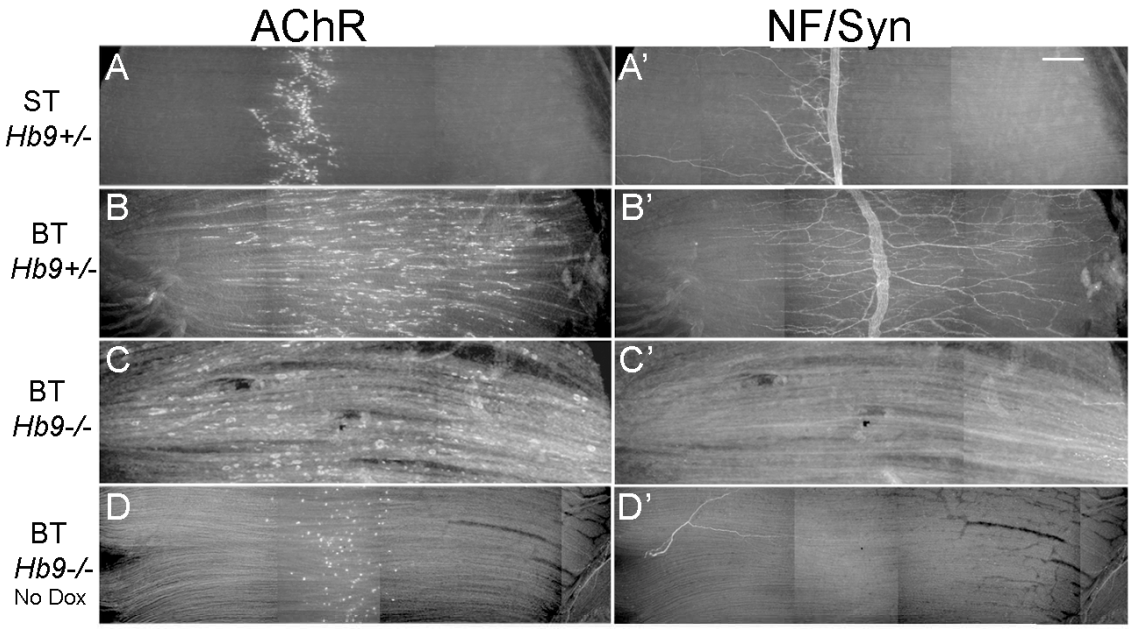
AChR
NF/Syn
A
A'
ST
Hb9+/-
B
B'
BT
Hb9+/-
C
C'
BT
Hb9-/-
D
D'
BT
Hb9-/-
No Dox

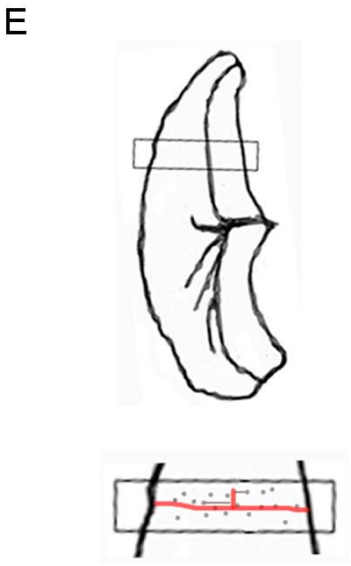
E

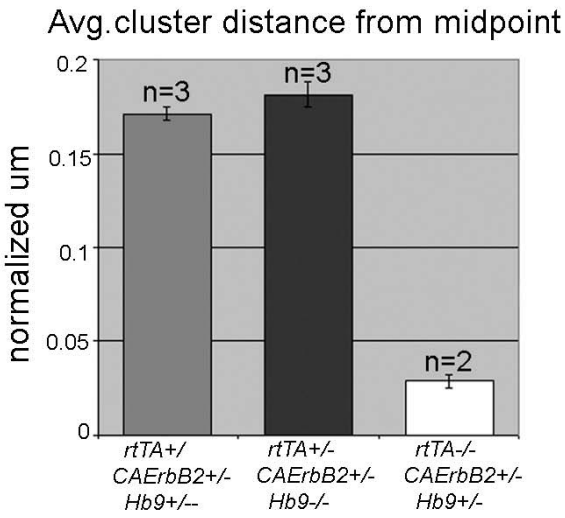
F
Avg.cluster distance from midpoint
normalized um
0.2
0.15
0.1
0.05
0
n=3
n=3
n=2
rtTA+/
CAErbB2+/-
Hb9+/--
rtTA+/-
CAErbB2+/-
Hb9-/-
rtTA-/-
CAErbB2+/-
Hb9+/-

Figure 2.7. Distributed pattern of AChR clustering is nerve-independent. (A-D') Whole mounts of diaphragm muscle from E18.5 embryos were labeled for axons/nerve terminals and AChRs as above. Epifluorescence microscopy was used to collect images that were aligned into montages to show the distribution of AChR clustering from end to end of diaphragms. (A) ST animals displayed central pattern of AChR clustering and (A') corresponding co-localization of central nerve bundle and nerve terminals. Scale bar = 50μm. (B) BT animals had cluster distribution that was previously demonstrated (Fig 3), where clusters were located throughout the width of diaphragm muscle and where (B') neuronal outgrowth resulted in nerve terminals which spread throughout diaphragm muscle. (C) When BT animals were also Hb9 null, AChR clusters were also found throughout the width of diaphragm muscle and (C') motor axons are absent from muscle as previously described. (D) Diaphragm muscle from BT Hb9-/- embryo that was not induced with Dox. AChR clusters appear in a centrally localized band, that is slightly wider than in ST controls but much narrower than in BT Hb9-/- embryos that received Dox. (D') Nerve staining shows an absence of motor axons while a sensory nerve is visible. (E) Cartoon of hemi-diaphragm showing region of muscle used for images and determination of AChR clusters distribution. An enlarged cartoon below shows how cluster distribution was measured. Width of diaphragm was determined, then a fraction of that width was used to determine the height of measurement region. Distances of 20 individual clusters from the midpoint of each diaphragm were collected. (F) Histogram showing average cluster distance comparisons between several genotypes. For each genotype, 20 cluster distances were measured from each animal, making a total of 60 clusters for each of the BT genotypes and 40 clusters for the ST embryos (n=3 and n=2, respectively).

DISCUSSION

By transient expression of CAErbB2 selectively in developing muscle, we forced the nerve and muscle to engage in synaptogenesis without a central pre-pattern of AChR clusters or AChR transcription. A widely diffused distribution of synapses throughout the muscle resulted. Under the nerve-dependent model of synaptogenesis, this distribution would have been explained by the wide pattern of axonal sprouting induced by CAErbB2 expression. Yet, in the absence of the nerve, a very similar, muscle-dependent distribution of aneural AChR clusters was generated. This result is not readily explained by the nerve-dependent model. It, together with the significant proportion of aneural

AChR clusters observed shortly after Dox withdrawal, suggest that the muscle may be setting the site for initiation of synaptogenesis in our experimental paradigm.

What results would have supported the nerve-dependent model? Because AChR clusters were absent by E15.5, one possibility was that no AChR clusters would have re-appeared by E18.5 in BT Hb9-/- mice. That is, all new AChR clusters would be nerve-dependent. This was clearly not the case as many aneural AChR clusters formed in BT Hb9-/- embryos. Another possibility that would have supported the nerve-dependent model was that aneural AChR clusters that re-formed in BT Hb9-/- diaphragm were restricted to the central area of the muscle. That is, outside the central zone, only nerve-induced synaptogenesis would occur as a result of axonal sprouting. This was also not case as the distribution of aneural AChR clusters in BT Hb9-/- diaphragms from embryos that received Dox (Fig 2.7C), was much wider than that in diaphragms from BT Hb9-/- embryos that received no Dox (Fig 2.7D).

What is the molecular mechanism(s) underlying the central-to-diffused distribution of NMJs after transient CAErbB2 expression? Although the precise mechanism(s) involved remains unknown, we suggest the following: (i) As shown in Fig 2.5, CAErbB2 expression led to relatively-uniform, high AChR mRNA expression throughout the muscle fibers by E15.5. This suggests that by expressing CAErbB2, we simply widened the transcriptional pre-pattern of AChR, and presumably other postsynaptic genes, from the central zone to the entire muscle fiber length. After Dox was withdrawn and CAErbB2 levels went below an unknown threshold, the nerve and muscle engaged in synaptogenesis, apparently following the rules during normal development except that they had a much wider field to do so, set by the width of the transcriptional pattern. To us this seems the simpler and more likely mechanism. This interpretation raises the possibility that what sets the location and pattern of mammalian neuromuscular

innervation is the width and location of the postsynaptic transcriptional pattern. Consistent with this conclusion, sensory and motor neuron conditional neuregulin-1 mutant mice display exuberant axonal sprouting of the phrenic nerve, yet show a central narrow band of AChR clustering and AChR transcription in their diaphragm (Yang et al., 2001). One NMJ per muscle fiber is the norm for most mammalian muscles. However, there are examples of multiple-innervated muscles such as the extraocular and laringeal muscles (cf. Khanna et al., 2003). Although, technically challenging, it would be interesting to examine the AChR clustering and transcriptional patterns in those muscles during development. Perhaps, multiple "pre-patterns" would also be observed. (ii) CAErbB2 expression could also both stimulate the production of muscle-derived axonal sprouting factors and/or inhibit the synthesis of adhesion molecules that normally stop the axon from growing beyond the central zone. This would only account for the exuberant axonal growth, not for the induction of AChR clustering, as the experiment with the BT Hb9-/- mice showed that the muscle itself can account for the latter. (iii) It is possible that by expressing CAErbB2 we altered the normal timing and expression of the endogenous muscle differentiation program. In this context, MyoD-/- mice display a diffused pattern of neuromuscular innervation that is evident beginning at E15.5 and persists into the adult (Wang et al., 2003). However, unlike our CAErbB2-expressing mice, in MyoD-/- mice, AChR clustering per se was not abolished at any time. The spatial pattern of AChR transcription was not studied in these mice.

In conclusion, we sought to provide a test in mice for the two models of neuromuscular synaptogenesis that have been proposed from prior studies in mice and zebrafish. Our results appear to support the muscle-dependent, pre-pattern model as the presence of the nerve seems unnecessary to generate the widely diffused innervation pattern we observed in mice transiently expressing CAErbB2.

CHAPTER 3

Additional evidence supporting muscle-dependent patterning

In the previous chapter, data was presented which has been submitted for peer-reviewed publication. In this chapter, I provide additional evidence collected that supports our claim that muscle plays an important role in development of the postsynaptic specialization, and that it does so in a manner that is nerve-independent.

Phenotype and postnatal survival of CAErbB2 pups

Activation of CAErbB2 was shown to eliminate AChR clusters from muscle, and was shown to be embryonic lethal when induced throughout gestation. Our goal in this study was to take advantage of the reversibility of our tet-on induction system to test two previously proposed models for synapse formation at NMJs. This was accomplished by withdrawl of doxycycline-containing food during gestation to allow AChR clustering to occur. Transgenic mice with disrupted NMJ formation die at birth due to the loss of synaptic function in the diaphragm that is necessary for breathing. BT (rtTA+/- ; CAErbB2 +/-) animals with a transient induction of CAErbB2 from E11.5 to E15.5 are born living, however due to differences in expression levels in skeletal muscles they display a phenotype that prevents coordinated movement or nursing. BT animals are born with a strong curvature to their bodies, and they appear unable to uncurl from this position. In addition, their arms are extended and do not move (Fig. 3.1). These animals die between 24 and 48 hours after birth, fail to nurse properly and have little, if any, milk in their stomachs during this period.

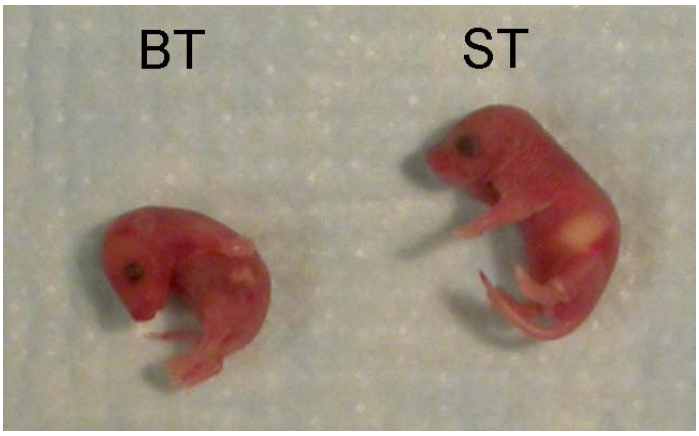

Figure 3.1. Experimental animals have limited movement and do not thrive. Two P0 littermates. The control, ST pup shows a normal body posture as well as the ability to right itself when rolled onto its back. In addition, this pup appears to have nursed due to the visible milk in the stomach. In contrast, the experimental, BT pup has a curved posture with arms that appear to be extended next to the body. These neonates are unable to uncurl their bodies or turn themselves if rolled onto their backs.

Expression profiles of reporter gene in arm and diaphragm of embryos

Previous work from our laboratory showed that expression of the CAErbB2 occurred at different levels in various skeletal muscle (Ponomareva et al., 2006). Because surviving BT pups showed an inability to move their limbs or nurse, but were clearly capable of breathing and thus survived at birth, I assayed luciferase reporter activity in the arm muscle and diaphragm muscle of pups during the recovery period, from E15.5 until birth. As expected, levels of luciferase reporter activity decrease between E15.5 and P0, but luciferase activity in arm muscles was substantially higher than in diaphragm muscle. This is consistent with the notion that while diaphragm appears to have synaptic function restored, other skeletal muscles may not have functioning synapses due to high remaining levels of CAErbB2 expression.

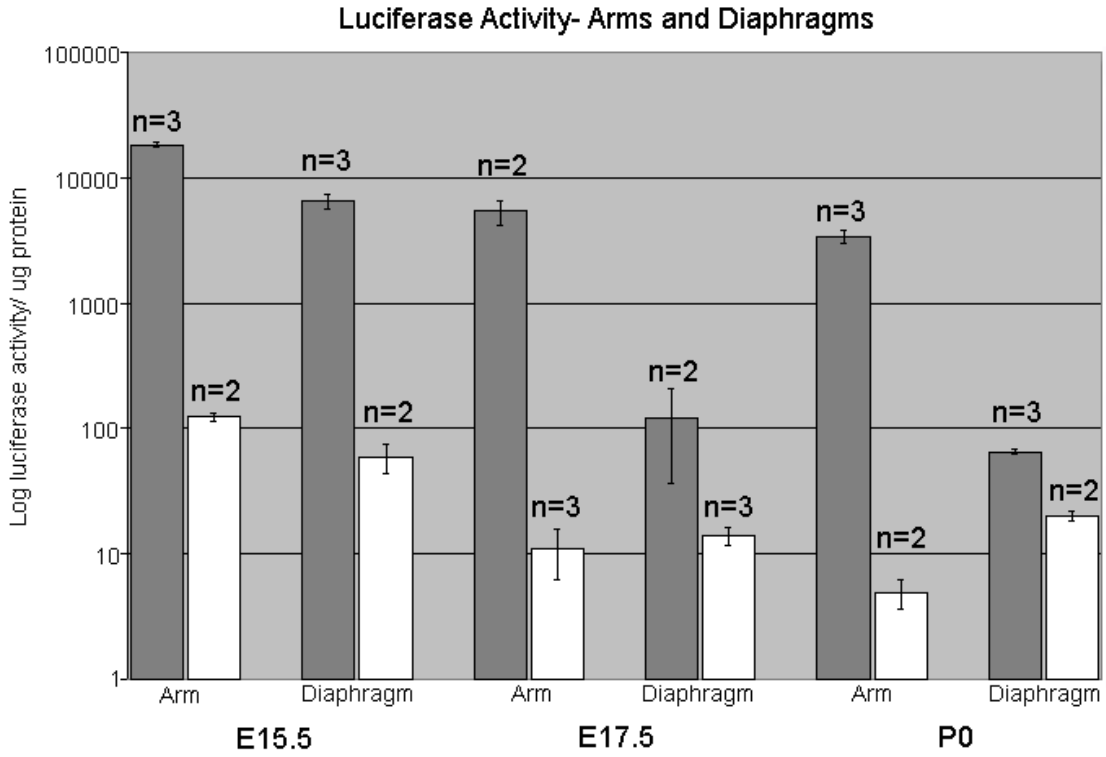

Figure 3.2. Luciferase activity is much higher in arms relative to diaphragms, and remains high at birth. Following doxycycline administration from E11.5- E15.5, luciferase activity is high in arm muscle compared to diaphragm, even during extinction period. Luciferase assay was performed using extracts from arm muscle and diaphragm muscle at 2 embryonic time points, and just after birth. The levels of luciferase activity is more than 3 times higher in arm than diaphragm at the time of doxycycline withdrawl, and activity in diaphragm declines rapidly. Levels of activity in diaphragm are near to that of ST control background by E17.5.

Synaptic markers present in distributed synapses

A number of postsynaptic proteins are present at the postsynaptic specialization, either clustered with or near the AChRs. In order to further determine whether restored synapses in BT neonates were similar to those which develop normally during embryogenesis, I did whole mount immunostaining for synaptic elements. Sections of diaphragm muscle were labeled with antibodies for MuSK and Rapsyn. In addition, we looked at the presence of acetylcholinesterase, an enzyme localized to the

synaptic cleft. All three markers were present at qualitatively normal levels in distributed synapses from sections of BT diaphragm muscle (Figure 3.3).

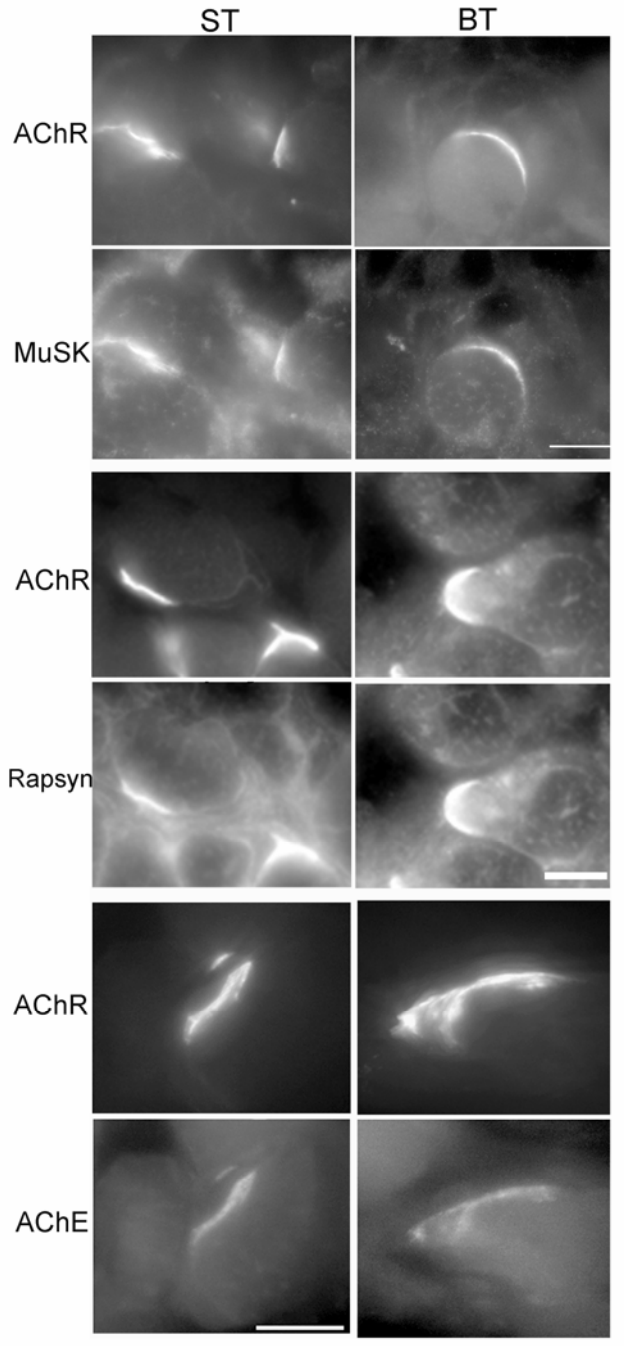

Figure 3.3. Synaptic markers are unchanged at distributed synapses. Diaphragm muscle of P0 ST and BT animals was flash frozen and cryosectioned for slide mounting. Sections were labeled with antibodies to MuSK (A', B') or Rapsyn (C', D') and co-labeled with fluorescein conjugated α-BXT (A, B, C, D, E, F). Sections of ST and BT were also labeled with Texas-Red conjugated fasciculin to label acetylcholinesterase (E', F'). Synaptic markers seem to be present at similar levels and localizations whether synapses were formed normally during development (ST) , or at a later developmental time and outside of the central zone (BT). Scale bar = 10μm.

Examination of tSCs in distributed synapses

Previously published results showed that activation of CAErbB2 in glial cells resulted in a reactive Schwann cell phenotype, where tSCs sprout and extend processes (Hayworth et al., 2006). To ensure that neuronal outgrowth was not in response to paracrine activation of signaling in tSCs or a reactive response, I crossed a mouse line into our signaling system. This forth transgenic line contains an S-100 promoter upstream of green fluorescent protein (GFP) cDNA to identify tSCs at synapses. We were able to compare synapse organization in control and experimental animals using this system. Females used in these experiments were rtTA +/- and GFP +/- or GFP +/+. We observed no qualitative changes in the appearance or number of tSCs at synapses after transient CAErbB2 induction (Fig. 3.4).

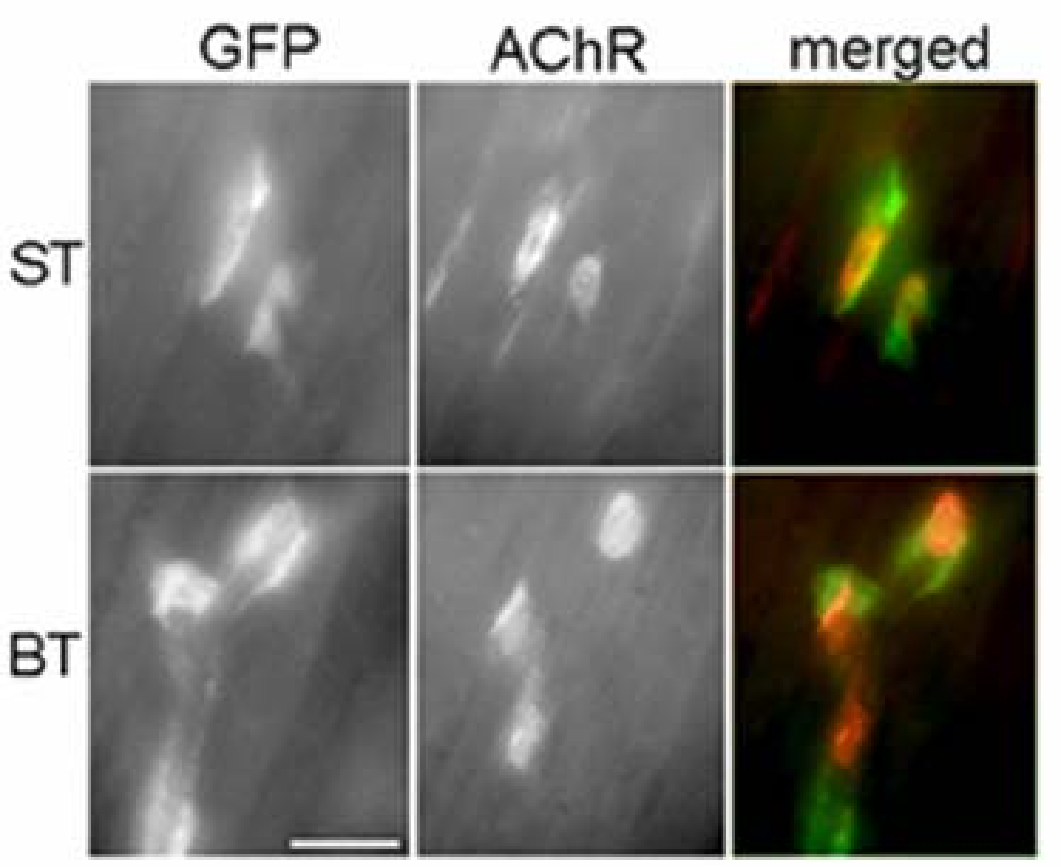

Figure 3.4. tSCs are present at distributed synapses. Whole mounts of diaphragm muscle from E18.5 embryos were labeled for AChRs as previously described. Distributed clusters from BT animals were compared to those in ST, control animals. (A) tSCs are seen to colocalized with AChR clusters (A'). The merged image showing their colocalization is to the right. (B) tSCs in animals with CAErbB2 signaling are similar to those in control animals, and receptor labeling shows clusters colocalize with tSCs (B'). The merged image to the right shows this colocalization. Scale bar = 20μm.

Comparisons of AChR cluster areas when phrenic nerve was absent

In addition to looking at synaptic factors in distributed synapses, we wondered if the clusters formed in the absence of nerve would be similar to those formed at distributed synaptic sites in recovered animals. Animals were generated that were heterozygous for rtTA and Hb9 disruption, and who were either CAErbB2 +/+ or +/-. Males and females with this genotype were crossed to generate experiemental progeny

without innervation of the diaphragm by motor neuron. AChR cluster area in animals with no phrenic innervation was statistically similar to those in the presence of nerve. This supports the notion that the muscle fibers are competent to form AChRs in a nerve-independent manner.

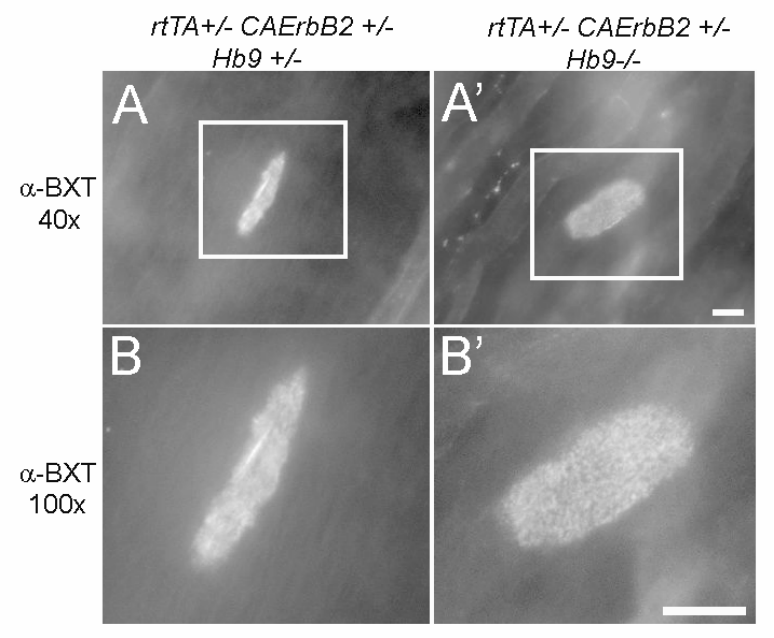

Figure 3.5. Cluster area was similar in animals who lacked neuronal innervation. Diaphragms of E18.5 embryos were dissected and labeled with fluorescein-conjugated α-BXT. Epifluorescence microscopy was done, and images captured with a high powered objective lens were used to quantify the area of muscle surface occupied by AChR clusters. Cluster area was defined using the Metamorph software tool (Molecular Devices). Clusters were first selected using a 40x objective (A, A') and then a 100x oil objective was used to examine the region of interest (B, B', white box in upper frames). Area of 10 AChR clusters from each genotype animal were compared using students t-test. No difference between cluster area was found in the absence of innervation (P=0.0160, students t-test, p=0.05). Scale bar =5μm

AChR cluster distribution in the absence of phrenic nerve

Initial examination of cluster distribution was done using a method where hemi-diaphragm width was determined, and three regions of equal area were defined with respect to full width of the hemi-diaphragm. The number of clusters found in each of the

three regions was quantified and compared. Clusters formed only in the central third of muscle in the animal that was BT and Hb9 -/- but received no dox, while only one cluster was seen outside the central region in animals that were ST and Hb9+/?. In animals who were BT and either Hb9 +/? or Hb9-/-, distributed clustering was seen, and clusters were distributed within all three regions (Fig. 3.6). More clusters were observed in the central third in these animals, with between 40 to 60 percent of clusters found in the central third of muscle. The balance of clusters had formed on either side of this central zone of muscle. Due to the similarities between cluster distribution in BT animals, I used an alternative method of cluster analysis which allowed statistical comparison of variances between clusters in animal with phrenic innervation and those lacking diaphragm innervation (Fig. 2.7).

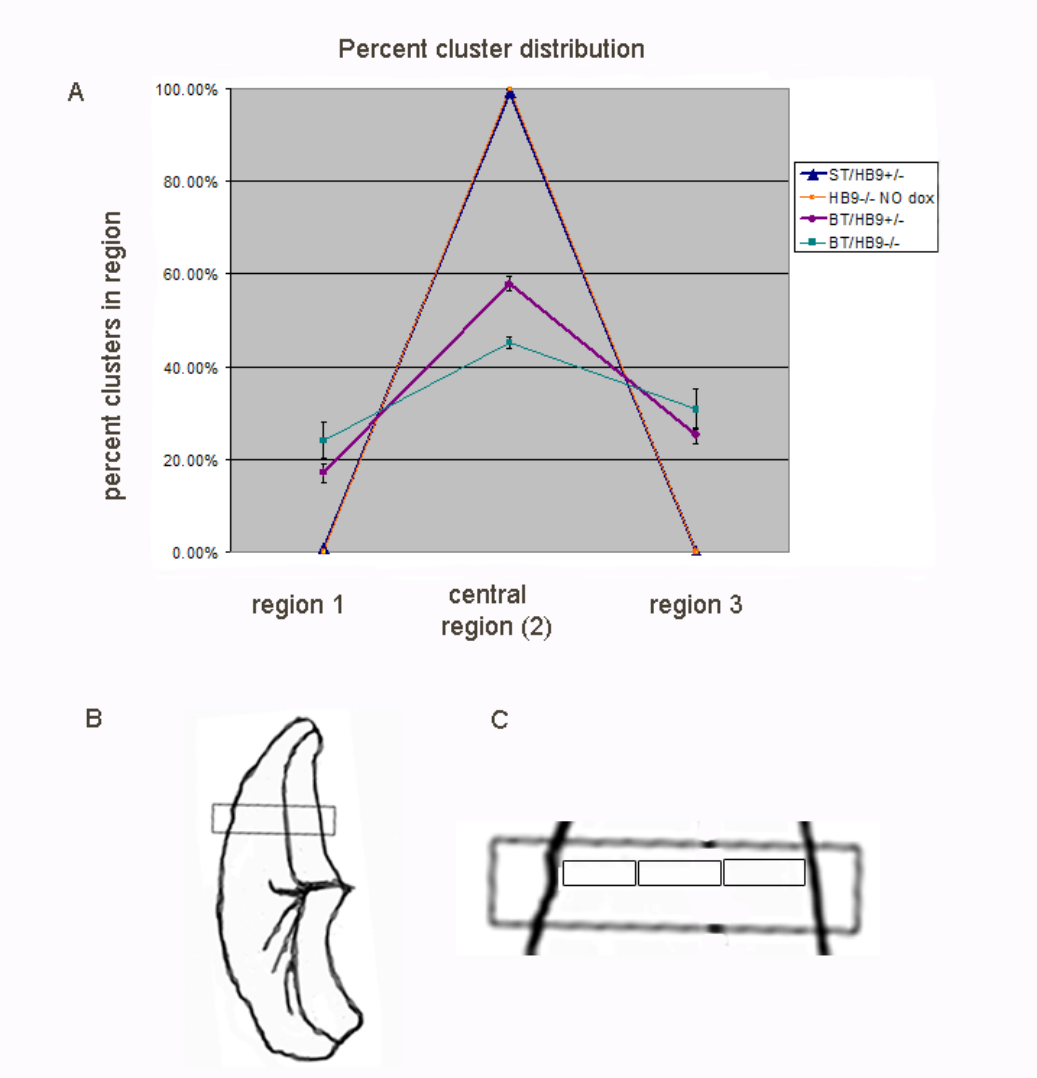

Figure. 3.6. Distributed clusters occur across the width of diaphragm and are similarly distributed. Whole mounts of diaphragm muscle were processed and aligned as described previously (Figure 2.7). (A) A dot plot was made to show the percentage of total clusters that were localized to each third of hemi-diaphragm. Control animals were ST/Hb9+/? or BT/Hb9-/- who were not administered doxycycline during embryogenesis. All AChR clusters were present in the central third of this muscle as opposed to the distributed localization that occurs following transient expression of CAErbB2. As seen in figure legend, 3 control animals were compared to 3 animals who were BT and had phrenic innervation of the diaphragm and 3 animals without motor neuron innervation of diaphragm. (B) Region of hemidiaphragms were selected for analysis, and (C) three rectangle of equal size were placed and used for during analysis.

CHAPTER 4

General discussion and future directions

MAJOR FINDINGS

The main purpose of this study was to test the two major models for NMJ synapse formation. Our work supports a muscle-dependent, pre-pattern model of synapse formation, where muscle is competent to pattern synapses during embryonic development in a nerve-independent manner. I first showed that we could eliminate AChR pre-pattern, then restore clusters and allow the formation of synapses in diaphragm muscle of murine embryos. Examination of diaphragm muscle from recovering pups at each day of the recovery period allowed characterization of synapse formation during the recovery period. I showed that synapse formation was possible in recovered animals, and that synapses were formed both in the endplate region and outside the customary region of receptor subunit transcription and receptor clustering, in areas of the muscle where synapses would not ordinarily form. I also found that synapses were not concentrated in any area of the diaphragm, but had formed in a widely diffused distribution throughout the diaphragm muscle. Functional synapses formed rapidly in our experimental animals, within four days after withdrawal of inducing food which contained doxycycline. This rapid synapse recovery may have been facilitated by the high levels of AChR transcription that were activated during CAErbB2 signaling. When additional synaptic elements were examined, no qualitative alterations were visible in experimental animals which suggests that other factors necessary for synapse formation are present in this muscle and cluster rapidly once levels of CAErbB2 signaling are reduced. I determined that additional postsynaptic elements and proteins were not altered after CAErbB2 activation. Terminal Schwann cells did not appear altered after transient CAErbB2

signaling in muscle, as at E18.5 were associated with recovery synapses. Rapsyn, MuSK and acetylcholinesterase were also found at synapses in recovered animals, and appeared qualitatively similar to their counterparts at control synapses. Measurements of cluster area showed that clusters in animals with CAErbB2 were similar to those which formed normally during development. My results demonstrate that the entire length of muscle fiber is capable of forming synapses that are functional and similar to those that form during normal embryogenesis.

EXPLANATIONS FOR AXONAL SPROUTING

If my work had supported the classical or nerve-dependent model of synaptogenesis, I could have explained the broad distribution of clusters as the result of extensive axonal sprouting that was activated following CAErbB2 expression. This was not the case since even in the absence of nerve, a similar distribution of aneural AChR clusters was observed. Since this distributed pattern formed even without neuronal factors, it cannot be explained by the classical model. I also detected aneural AChR clusters shortly after Dox withdrawal which provides additional evidence that clusters form in the absence of nerve. My data suggest that the clusters form first and then the nerve contacts them. This would be consistent with reports from observations in the zebrafish that showed nerve forming contacts with clusters as it extended through the myotome of zebrafish. In addition, while aneural clusters were evident within 24 hours following dox-withdrawal, the axons continued to extend throughout muscle. Since I was unable to follow the projection path of neural extension through the muscle, we could not say definitively whether axons made contact with clusters and therefore whether this contact caused the nerve to stop growing and form a synapse at the cluster site. One possible explanation for the continued nerve extension after clusters form may be that the aneural AChR clusters may be nascent clusters and not yet be associated with additional

postsynaptic proteins such as Src-family kinases, MuSK or rapsyn which may be a necessary part of a "mature" or stable AChR cluster, and as such may not be capable of response to neurotransmitter. Thus, the neuronal outgrowth that we observe following cluster elimination may be due to the absence of other factors needed for synapse formation or that would allow synaptic response or activity. Another explanation for the neural outgrowth that we observe may be the lack of activity. Previous studies have shown that axonal sprouting was observed following activity blockade or denervation (Duchen and Strich, 1968; Srihari and Vrbova, 1978; Brown and Varkey, 1981; Holland and Brown, 1981; Zhao and Nonet, 2000). Newly formed clusters may not only be immature, but may also be incapable of binding neurotransmitter which could simulate blockade or denervation. If either of these possibilities were true, the nerve could make transient contact with the cluster but might continue to extend through muscle seeking a cluster that is stabilized or complexed with additional postsynaptic proteins, and capable of response to neurotransmitter. An alternative explanation for the neuronal outgrowth seen with CAErbB2 expression is that sustained ErbB2 activation might stimulate the production of muscle-derived axonal sprouting factors and/or inhibit the synthesis of adhesion molecules that normally stop the axon from growing beyond the central zone.

CHALLENGING THE CLASSICAL MODEL

Two experimental outcomes would have supported the classical, nerve-dependent model. Because AChR clusters had been eliminated by E15.5, one possibility was that AChR clusters would not have re-formed in Hb9-/- mice. That would have suggested that the AChR clusters we had observed by E18.5 in BT animals were the result of nerve-secreted factors. I did not find this since many aneural AChR clusters formed in BT Hb9-/- embryos. I might have also discovered that the aneural AChR clusters that re-formed in BT Hb9-/- diaphragm would be restricted to the central area of the muscle.

This result would have suggested that if clustering occurred without neuronal influence, it could be the result of signaling regional to the central zone, signaling that was not eliminated but perhaps only suppressed during CAErbB2 activation. I did not find clustering in the center of muscle but the distribution of aneural AChR clusters in BT Hb9-/- diaphragms from embryos that received Dox was much wider than the cluster distribution in diaphragms from BT Hb9-/- embryos that received no Dox. That the distributed pattern was present regardless of whether the diaphragm was innervated suggests that what normal developmental patterning was altered when CAErbB2 signaling occurred and was not due to factors secreted from the motor axon.

PROPOSED EXPLANATIONS

While this study has provided additional evidence showing that the nerve is not necessary for cluster formation during development, I present new evidence that synapse formation is not dependent on a central pre-pattern of clusters as we have altered transcriptional patterning and AChR cluster localization, and I have shown that synapses are not limited to a central region of muscle but can be formed anywhere on a muscle fiber. While I did not determine the precise mechanism involved in the change from central to diffused distribution of synapses seen following transient CAErbB2 expression, I suggest the following possibilities:

Transcriptional patterns are key for determining the site of synapse formation. The concentration of postsynaptic proteins at the NMJ requires the local synthesis of receptor subunits and postsynaptic proteins. While I found increases in transcription of AChR-α subunit with induction of the CAErbB2, the use of a muscle specific promoter induced CAErbB2 signaling throughout the length of the muscle fibers. This is in contrast to the normal developmental transcription pattern, where high levels of AChRs would be

concentrated at the end-plate zone during the time of synapse formation. Since CAErbB2 expression led to relatively-uniform, high AChR mRNA expression throughout the muscle fibers by E15.5, by transient expression of CAErbB2 I dramatically altered the transcriptional pattern of AChRs and presumably other postsynaptic genes, from the central zone to the entire muscle fiber length. Following dox withdrawal, CAErbB2 returned to levels below an unknown threshold and the nerve and muscle engaged in synaptogenesis in a distribution that was determined by the transcriptional distribution. To me, this seems the simpler and more likely mechanism. This interpretation raises the possibility that what sets the location and pattern of mammalian neuromuscular innervation is the width and location of the postsynaptic transcriptional pattern.

By expressing CAErbB2 we altered the normal timing and expression of the endogenous muscle differentiation program. Since normal transcriptional patterning shows AChRs clustered in the myotubes that differentiated earliest during development, it is possible that simple elimination of pre-pattern of clusters at ~E12 or E13 allows myotubes that are continuing to differentiate between ~E12 and E15.5 to be have developed to a point that allows transcription to occur throughout the fiber. In short, I simply delay the onset of transcription until the whole fiber is fully differentiated that in turn allows clusters to form throughout the fiber.

FUTURE DIRECTIONS

In this study, I have determined that muscle plays an important role determining the site of synapse formation during development, and we have provided evidence that supports the muscle-dependent model of NMJ formation in mammalian development. While I could effectively characterize the process of synapse formation during the recovery period, I could not visualize this in-vivo to determine if we observed nerve

seeking a pre-existing AChR in the diaphragm muscle. Since zebrafish provide an ideal model system for in-vivo imaging during development, it is possible that they could be used to determine whether similar alterations in transcriptional patterning could result in a distributed pattern of synapse formation in zebrafish mytome.

In addition, while I refer to the induction of CAErbB2 receptor signaling as transient, due to the ligand-independent mechanism of ErbB2 signaling we can assume that its activation is sustained with respect to activation of the downstream signaling cascade. Some reports have demonstrated that transient and sustained activation of ErbB receptors may result in differing MAPK signaling outcomes (Heasley and Johnson, 1992; Nguyen et al, 1993; Traverse et al., 1992). While this study did not address the signaling mechanism downstream of the CAErbB2 activation, additional work should be done to elucidate the pattern of MAPK activation following native ErbB2 activation.

Another helpful study would be an attempt to alter the transcriptional patterning of myotubes without the CAErbB2 signaling to verify if this is the mechanism that enables synapse formation throughout the myotome.

CONCLUSION

In conclusion, my work sought to provide a test in mice for the two models of neuromuscular synaptogenesis that have been proposed from prior studies in mice and zebrafish. My results support a muscle-dependent, pre-pattern model as the presence of the nerve seems unnecessary to generate the widely diffused clustering pattern we observed in mice transiently expressing CAErbB2.

CHAPTER 5

Detailed Methodology

Transgenic mice

Two transgenic lines were developed containing cDNAs encoding a reverse tetracycline transactivator (rtTA) or a constitutively active ErbB2 receptor (CAErbrB2) (described in Ponomareva et al., 2006). The rtTA protein is ubiquitously expressed. The CAErbB2 construct was cloned with a muscle-specific promoter and a luciferase reporter sequence downstream of the ErbB2 sequence. Experiements testing the reformation of synapses/AChR clusters were done by crossing males which were homozygous for CAErbB2 with heterozygous rtTA females. This breeding strategy allowed single transgenic (ST, rtTA-/-; CAErbB2+/-) and bi-transgenic (BT, rtTA+/-; CAErbB2+/-) embryos to be generated as a result of each cross. The former (ST) served as control whereas the latter (BT) were the experimental animals.

Experiments to test the models of NMJ formation using animals lacking innervation of the diaphragm were done using a third transgenic mouse line. Mice with a disruption in the Hb9 transcription factor were provided by S. Burden with permission from T. Jessell. Hb9 +/- males were crossed into an rtTA +/- CAErbB2 +/- background, in order to generate progeny with all three genes. During experimental crosses, triple transgenic animals (rtTA +/- ; CAErbB2 +/- or +/+ ; Hb9 +/-) were crossed to each other in order to optimize the number of offspring who might be both BT and homozygous for the Hb9 disruption (HB9 null).

In order to examine tSCs at synapses, a mouse line was provided by W. Thompson that expressed green fluorescence protein (GFP) under the control of S100 regulatory sequences (described in Zuo et al., 2004). This male was crossed with our

rtTA mice in order to produce crossing females who were GFP+/-; rtTA+/-. Females who were determined to be rtTA +/- and GFP +/- were crossed with homozygous CAErbB2 males, producing ST and BT progeny that had GFP-labeled Schwann cells.

Genotyping

The tip of a toe from each animal was collected and digested to isolate genomic DNA. A standard Phenol/Chloroform extraction protocol was used for genomic DNA isolations prior to 2006. An alternative method (eliminating Phenol-Chloroform extraction) was used beginning in January, 2006. Lysis buffer for digestion of toe tip was prepared at the follow stock concentration, and stored at room tempreature: 1M Tris-HCL (pH 8.5), 500mM EDTA (pH 8.0), 20% SDS, 5M NaCl, 20 mg/ml Proteinase K. 500ul of lysis buffer was added to the tissue in a microcentrifuge tube and the tube was incubated overnight at 55 ◦C. On the second day, tubes were spun for 5 minutes at the highest speed to pellet undigested debris. Supernatant was extracted and placed into new microcentrifuge tube and one volume of isopropanol was added to each tube. The tubes were inverted and shaken vigorously, by hand for about one minute or until a DNA precipitant was observed. Samples were then spun at highest speed for 10 minutes and upper volume of liquid in the tube was removed carefully with a pipette tip, leaving only a few drops of solution with pelleted DNA at the bottom of tube (the pellet was not always visible or adherent to tube, so this procedure was done with care not to lose pellet). 500ul of 70% EtOH was added to each tube and tubes were spun at high speed for about 1 minute. EtOH was removed, and tube was allowed to dry at room temperature for 5 minutes. When dry, the pellet was resuspended in 400ul of filtered, autoclaved water which had been treated with exposure to UV light for at least 10 minutes. 1 ul of DNA was used in polymerase chain reactions (PCRs) for gene detection.

Standard PCR reactions were run using a thermocycler. Genotyping reactions were done using FastStart Taq DNA polymerase (Roche). Primers used were as follows:

(i) rtTA: Forward, 5'-AGAGCACAGCGGAATGACTT-3'.

Reverse: 5'-GCCTGACGACAAGGAAACTC-3'.

(ii) CAErbB2:IRES:Luciferase: Forward: 5'-CTTCTTCGCCAAAAGCACTC-3'.

Reverse: 5'-CACACAGTTCGCCTCTTTGA-3'.

(iii) detection of Hb9 disruption (does not distinguish homozygous):

Forward: 5'-CCGGTGACCGTGCAAAACAGGCTCTA-3'.

Reverse: 5'-CTTCCAGGGCGCGAGTTGATAGC-3'.

(iv) detection of full Hb9 deletion: Forward: 5'-TGCACAGGCGGCTCTCTATGG- 3'.

Reverse: 5'-CCACAGCTCGCTAGGAGGTGAG-3'.

(v) GFP: Forward: 5'-AATCGAGTTGAAGGGCATTG-3'.

Reverse: 5'-GCCGATTGGAGTGTTCTGTT-3'

Doxycycline induction of CAErbB2

Standard rodent food was ground until smooth using a small coffee bean grinder. For each 1 gram of powdered rodent food, 6 grams of doxycycline (Dox, Sigma, St. Louis, MO) and 5% sucrose were dissolved in small volume of water. Desired quantity of rodent food was measured and place in a glass beaker. Dox, sucrose and water were mixed in an erlenmeyer flask and added to the rodent food. Gloved hands were used to mix the food well, and additional water was added as needed. Food was ready to pellet when moist but not runny. Small cylindrical pellets were formed by hand, and wrapped in plastic wrap. Food was kept at 4◦ C until ready to administer. Dox-containing food was given to pregnant dams at the time indicated in the text. Dox was delivered to embryos via ingestion by the mother, and passed to embryos through the placenta. All

animal experiments were approved by the University of Texas Institutional Animal Care and Use Committee.

Dissection and fixation of embryonic and P0 animals

Embryo dissections were done by euthanizing an expectant female, and removal of the uterine horn. After uterine horn was removed, it was placed in a sterile PBS bath (shallow glass beaker), and placed on ice. Individual amniotic sacs were removed, and pups were placed into a round bottom tube containing 3 mls Paraformaldehyde (PFA). At the time of dissection, tail tips were removed and processed as described above for genotyping. Embryonic day (E) 14 and E15 whole embryos were fixed in 4% paraformaldehyde (PFA) at 4◦C overnight. The next day, concentrated PFA was replaced with 0.4% PFA until diaphragm dissection (1-4 days following embryo removal). Older (E16, E17, E18) embryos and neonates were fixed in 2% PFA and replaced with 0.2% PFA as described above. After birth, postnatal animals were decapitated and bodies were placed into 4% PFA for fixation. The second day, 4% PFA was removed and replaced with 0.4% PFA until needed.

Dissection of ribcage and diaphragm

Following fixation of embryos, the ribcage section of the torso was collected and trimmed such that internal organs were removed and diaphragm muscle was visible. Additional ribs and connective tissue were removed so that a few ribs remained, which helped hold the diaphragm taut. This strategy allowed fluid to circulate around and into the remaining ribcage. The ribcage was placed into low concentration PFA (0.2% or 0.4%) in multi-well tissue culture dish (12 well) until ready to further process. Later the same day but prior to antibody staining, diaphragm muscle was liberated from the rib cage. Small specimen pins were used to the pin ribcage onto sylgard resin at the bottom

of a glass Petri dish. Pins were carefully inserted through intercostal muscles and connective tissue to suspend the ribcage during dissection. The spinal cord was removed, then working from one side, small scissors were used to cut carefully along the side edge of diaphragm, between diaphragm and ribcage. Once the ventral region of diaphragm was detached from the sternum, pins were placed into connective tissue in the center of diaphragm to continue to hold it in place. When entire diaphragm was detached, it was placed into a multi-well dish for washing. PFA was removed and replaced with PBS before immunohistochemistry was performed.

Extraction of protein from muscle

For protein extraction, animals were dissected as described except embryos were not placed in fixative. Rather, diaphragm and arm muscle were dissected immediately and rapidly frozen in liquid nitrogen. Samples were placed in microcentrifuge tubes and stored at -80 ◦C. At the time of protein extraction, muscles were thawed on ice and homogenized in between 100-250 ul Luciferase Cell Culture Lysis Reagent (Promega, Madison, WI). A glass homogenizer was used to grind tissue, and tissue grinding was done with homogenizer resting on ice during the process. Once the tissue was homogenized and no remaining clumps of tissue were observed, samples were placed into a microcentrifuge tube and centrifuged at 4°C. Samples were stored immediately until determination of protein concentration using a Bradford Assay.

Assay of luciferase reporter activity

Twenty microliters of cleared lysate was added to a Chromalux flat bottom plate (Dynex). Luciferase activity assay was performed on a Dyanex MLX Microplate Luminometer using 40 µl Luciferase Assay Reagent (Promega, Madison, WI) with a total

read time of 10s. Total light units obtained from reading were normalized to total protein content determined by the Bradford assay (Biorad, Hercules, CA).

Immunohistochemistry

After dissection of diaphragms, immunohistochemistry was performed on whole diaphragms. Washes and antibody incubations were done in multi-well tissue culture dishes. Muscle tissue was washed twice with 1x PBS for 5 minutes duration. Following initial washes, any remaining connective tissue that was observed on the surface of muscle tissue was removed with forceps. Samples were then washed with 1ml of 0.1M glycine in 1x PBS for 15 minutes, rinsed with 1x PBS for 5 minutes on shaker, then washed for 5 minutes with 1X PBS containing 0.5% Triton X-100 (PBS-T). PBS wash was removed and incubation buffer containing primary antibodies was added. Incubation buffer was PBS-T with 2% BSA added. Axons and nerve terminals were labeled with polyclonal rabbit anti-neurofilament at 1/500 (Chemicon, now Milipore , Billerica, MA) and anti-synaptophysin at 1/200 (Zymed, now Invitrogen, Carlsbad, CA). Samples were incubated with gentle shaking overnight at 4 ◦C. The following day, primary antibody solution was removed and samples were rinsed with PBS, then washed 3 times for 20 minutes each time in PBS-T. Secondary antibodies were added to incubation buffer, and then samples were protected from light and incubated for 3 hours at room temperature or at 4 ◦C overnight. Rhodamine-conjugated, anti-rabbit IgG secondary (Jackson Immunoresearch, West Grove, PA) was used to visualize neuronal markers, while acetylcholine receptors (AChRs) were labeled with fluorescein-α-bungarotoxin (BTX, Molecular Probes, Eugene, OR) at 1/1000. Following antibody incubation, samples were washed as after primary incubation, then left in PBS overnight.

The following day, samples were mounted in Vectashield (Vector Labs, Burlingame, CA) and viewed in a Eclipse E-1000 fluorescence microscope (Nikon) equipped with filters selective for either fluorescein or rhodamine.

Preparation of muscle sections

Sections were also made of P0 diaphragm muscle for immunohistochemistry. P0 pups were decapitated and diaphragm muscle was dissected as previously described with the exception of the removal of ribs and liver underneath the diaphragm muscle. Ribs were fully removed during dissection, and diaphragm and liver were placed into Tissue-Tek embedding media, then frozen in liquid nitrogen. A microtome cryostat was used to slice the diaphragm into Transverse sections (BT muscle, some ST muscle) or Coronal sections (some ST muscle). Sections were 16 um thick and were placed on charged glass slides in serial sections. Slides were stored with dessicant at -80 ◦C until used. Slides were removed from the freezer in pairs and thawed on benchtop for a few minutes until excess water could be blotted from slide surface with a kimwipe. Slides were placed into the inverted lid of a pipette tip box, and 1% PFA was pipetted over the tissue. PFA was dumped off after 10 minutes and slides were dipped into a glass slide washer containing PBS-T. Slides were washed 3 times for 20 minutes each, then edges of slides were blotted dry and a pap pen was used to surround area containing tissue sections. After the pap line was dry, slides were placed back into slide washer and blocked for one hour in PBS-T containing 0.3% Triton and 1% BSA. Slides were then removed from the washer and placed face-up, on top of an empty pipette tip box containing water in the lower chamber. Antibodies were added to 500ul PBS-T/BSA solution (per slide), and the solution was gently loaded onto top of the sections. The lid of the box was replaced and the box was incubated at 4 ◦C. overnight. The following day, slides were removed and put into glass washers for 3 20 minute washes in PBS-T. Secondary antibodies were

added to PBS-T/ BSA solution and applied as described above. The pipette box was wrapped in foil, and incubated at room temperature for one hour. Following secondary antibody incubation, slides were briefly rinsed in PBS-T then washed 2 times for 30 minutes in PBS-T. following these washes, slides were washed 2 times for 5 minutes in PBS before mounting with vectashield mounting media and a coverslip. Slides were imaged as described for whole mount histochemistry. Sections were labeled with antibodies to MuSK and Rapsyn, and labeled with Cy-5 conjugated fasciculin or fluroescein conjugated α-BXT.

In situ hybridization

Dissection tools and equipment were rinsed in 3% hydrogen peroxide prior to use, and rinsed in DEPC treated water before using. All reagents used during dissection and fixing were prepared using DEPC treated water. Rib cages were dissected as described previously, and following dissection, the whole rib cage was placed in 4% PFA overnight. The following morning, rib cages were placed in 0.4% PFA. Each diaphragm was dissected from rib cage as previously described, then moved to small glass vial (scintillation vial). The diaphragms were washed 2 times in 1X PBS with 0.1% active DEPC for 15 minutes each wash. DEPC wash was removed and replaced with 5X SSC for a 15 minute wash. Samples were prehybridized in 50% Formamide, 5xSSC, 40ug/ml salmon sperm DNA for 2 hours in a 58 ◦C hybridization oven. Following pre-hybridization, the probe was added to new aliquot of pre-warmed prehybridization solution with a final probe concentration of 400ng/ml. Probe was hybridized with muscle for 40 hours. Following hybridization, a series of washes in SSC were done. The first wash was done using 2X SSC for 30 minutes at room temperature. The next wash was with 2X SSC for 1 hour at 65 ◦C. The final wash was in 0.2 SSC for 1 hour at 65 ◦C. The samples were then equilibrated for 5 minutes in “buffer 1” containing 100 mM Tris

and 150mM NaCl (pH 7.5). Muscle was then incubated overnight at 4 ◦C in buffer 1 containing 0.5% nonfat dry milk added, and with 1:5000 Anti-DIG-AP. The following day, samples were washed in buffer 1 all day with 3 to 4 buffer changes, and washed 2 times for 20 minutes in 100 mM Tris, 100mM NaCl and 50mM $MgCl_2$ (pH 9.5), with 1:1000 Tween added. Color reaction was set overnight by incubating in buffer containing NBT and BCIP.

A previously described probe for AChRα (Rimer et al., 2004) (Rimer et al., 2004) and a 1317 bp-probe for mouse AChRε cDNA (AChRε ISH2, kindly provided by S. Burden, New York University, NY) were labeled with digoxigenin, chemically hydrolyzed (Schaeren-Wiemers and Gerfin-Moser, 1993), and used for whole-mount in situ hybridization following a protocol originally described for tissue sections (Braissant and Wahli, 1998).

Confocal microscopy

High resolution, high magnification images were captured using a Leica SP2 AOBS Laser Scanning Spectral Confocal Microscope (Leica Microsystems). A 63X oil (HCX PL APO 1.4-.60 NA Blau CS) objective with digital zoom allowed captured images at approximately 120X magnification.

Regions of diaphragm muscle containing groupings of several synapses were first localized using a low power objective lens. High-power images were obtained where at least one cluster was visible "en face", i.e. oriented toward the viewer. Z stacks were 0.12 um thick. To measure postsynaptic area, stacks were rotated using the Metamorph software tool (Molecular Devices Corporation, Downingtown, PA) until one cluster of the region was visible en face. A maximal projection was generated from the stack and the border around the en face AChR cluster was thresholded. This was repeated for six en face clusters from each ST and BT animal. The area occupied by labeled AChRs was

measured and Students' t-test was done to determine whether cluster area differed between control and experimental animals.

Aneural AChR cluster analysis

Diaphragm muscle from E16.5, E17.5 and P0 was visually scanned using the 40x objective (NA 1.30, Nikon) in the widefield microscope described above. Three to five regions of lateral, normally extrajunctional zone were examined in BT samples, while 1-2 regions adjacent to the center of the muscle were examined in ST samples. In all cases, regions selected were either dorsal or ventral to region of phrenic nerve branching. Clusters in a given field were counted, and categorized as either nerve-associated (co-localized with nerve terminal staining) or aneural (not near a visible nerve terminal). Planes above and below the plane of focus for the AChR clusters were scanned to confirm the absence of nearby axonal processes.

Analysis of synapse / aneural AChR cluster distribution

Montages were created by aligning adjacent images of diaphragm muscle taken with the 10X objective (NA 0.30, Nikon) of the widefield microscope. All images were obtained from the region of diaphragm just ventral to the area where phrenic nerve branching occurs. The width of hemi-diaphragm was then determined by drawing a line across the width of the assembled collage.

For the analysis of synapse/cluster distribution described in Figure 3.6, three rectangles of identical dimensions were created in the region described above. Individual clusters were counted in each region, with regions being described as center third, or outside thirds.

For the analysis of synapse/cluster distribution described in Figure 2.7, the mid line of hemi-diaphragm width was marked on each collage along with a short line,

perpendicular to width line and extending above the width line for a distance of 1/30th of muscle width. The distance between synapses or distributed AChR clusters and the midline was measured and recorded. Sixty cluster distances were obtained from hemi-diaphragms of 3 embryos for each genotype. Analysis of variance was calculated using distance measurements normalized to the total measured width of hemi-diaphragm from each animal.

References

Altiok N, Bessereau JL, Changeux JP (1995) ErbB3 and ErbB2/neu mediate the effect of heregulin on acetylcholine receptor gene expression in muscle: differential expression at the endplate. Embo J 14:4258-4266.

Anderson MJ, Cohen MW (1977) Nerve-induced and spontaneous redistribution of acetylcholine receptors on cultured muscle cells. J Physiol 268:757-773.

Arber S, Burden SJ, Harris AJ (2002) Patterning of skeletal muscle. Curr Opin Neurobiol 12:100-103.

Arber S, Han B, Mendelsohn M, Smith M, Jessell TM, Sockanathan S (1999) Requirement for the homeobox gene Hb9 in the consolidation of motor neuron identity. Neuron 23:659-674.

Borges LS, Ferns M (2001) Agrin-induced phosphorylation of the acetylcholine receptor regulates cytoskeletal anchoring and clustering. J Cell Biol 153:1-12.

Braissant O, Wahli W (1998) A simplified in situ hybridization protocol using non-radioactively labeled probes to detect abundant and rare mRNAS on tissue sections. Biochemica 1:10-16.

Braithwaite AW, Harris AJ (1979) Neural influence on acetylcholine receptor clusters in embryonic development of skeletal muscles. Nature 279:549-551.

Brown WF, Varkey GP (1981) The origin of spontaneous electrical activity at the end-plate zone. Ann Neurol 10:557-560.

Cohen I, Rimer M, Lomo T, McMahan UJ (1997) Agrin-induced postsynaptic-like apparatus in skeletal muscle fibers in vivo. Mol Cell Neurosci 9:237-253.

Corfas G, Falls DL, Fischbach GD (1993) ARIA, a protein that stimulates acetylcholine receptor synthesis, also induces tyrosine phosphorylation of a 185-kDa muscle transmembrane protein. Proc Natl Acad Sci U S A 90:1624-1628.

Dahm LM, Landmesser LT (1991) The regulation of synaptogenesis during normal development and following activity blockade. J Neurosci 11:238-255.

DeChiara TM, Bowen DC, Valenzuela DM, Simmons MV, Poueymirou WT, Thomas S, Kinetz E, Compton DL, Rojas E, Park JS, Smith C, DiStefano PS, Glass DJ,

Burden SJ, Yancopoulos GD (1996) The receptor tyrosine kinase MuSK is required for neuromuscular junction formation in vivo. Cell 85:501-512.

Duchen LW, Strich SJ (1968) The effects of botulinum toxin on the pattern of innervation of skeletal muscle in the mouse. Q J Exp Physiol Cogn Med Sci 53:84-89.

Escher P, Lacazette E, Courtet M, Blindenbacher A, Landmann L, Bezakova G, Lloyd KC, Mueller U, Brenner HR (2005) Synapses form in skeletal muscles lacking neuregulin receptors. Science 308:1920-1923.

Falls DL, Rosen KM, Corfas G, Lane WS, Fischbach GD (1993) ARIA, a protein that stimulates acetylcholine receptor synthesis, is a member of the neu ligand family. Cell 72:801-815.

Ferns M, Deiner M, Hall Z (1996) Agrin-induced acetylcholine receptor clustering in mammalian muscle requires tyrosine phosphorylation. J Cell Biol 132:937-944.

Fertuck HC, Salpeter MM (1976) Quantitation of junctional and extrajunctional acetylcholine receptors by electron microscope autoradiography after 125I-alpha-bungarotoxin binding at mouse neuromuscular junctions. J Cell Biol 69:144-158.

Fex S, Thesleff S (1967) The time required for innervation of denervated muscles by nerve implants. Life Sci 6:635-639.

Finn AJ, Feng G, Pendergast AM (2003) Postsynaptic requirement for Abl kinases in assembly of the neuromuscular junction. Nat Neurosci 6:717-723.

Fischbach GD, Cohen SA (1973) The distribution of acetylcholine sensitivity over uninnervated and innervated muscle fibers grown in cell culture. Dev Biol 31:147-162.

Fischbach GD, Rosen KM (1997) ARIA: a neuromuscular junction neuregulin. Annu Rev Neurosci 20:429-458.

Flanagan-Steet H, Fox MA, Meyer D, Sanes JR (2005) Neuromuscular synapses can form in vivo by incorporation of initially aneural postsynaptic specializations. Development 132:4471-4481.

Frank E, Fischbach GD (1979) Early events in neuromuscular junction formation in vitro: induction of acetylcholine receptor clusters in the postsynaptic membrane and morphology of newly formed synapses. J Cell Biol 83:143-158.

Fuhrer C, Sugiyama JE, Taylor RG, Hall ZW (1997) Association of muscle-specific kinase MuSK with the acetylcholine receptor in mammalian muscle. Embo J 16:4951-4960.

Gautam M, Noakes PG, Mudd J, Nichol M, Chu GC, Sanes JR, Merlie JP (1995) Failure of postsynaptic specialization to develop at neuromuscular junctions of rapsyn-deficient mice. Nature 377:232-236.

Gautam M, Noakes PG, Moscoso L, Rupp F, Scheller RH, Merlie JP, Sanes JR (1996) Defective neuromuscular synaptogenesis in agrin-deficient mutant mice. Cell 85:525-535.

Flanagan-Steet H, Fox MA, Meyer D, Sanes JR (2005) Neuromuscular synapses can form in vivo by incorporation of initially aneural postsynaptic specializations. Development 132:4471-4481.

Glass DJ, Yancopoulos GD (1997) Sequential roles of agrin, MuSK and rapsyn during neuromuscular junction formation. Curr Opin Neurobiol 7:379-384.

Glass DJ, Bowen DC, Stitt TN, Radziejewski C, Bruno J, Ryan TE, Gies DR, Shah S, Mattsson K, Burden SJ, DiStefano PS, Valenzuela DM, DeChiara TM, Yancopoulos GD (1996) Agrin acts via a MuSK receptor complex. Cell 85:513-523.

Heasley LE, Johnson GL (1992) The beta-PDGF receptor induces neuronal differentiation of PC12 cells. Mol Biol Cell 3:545-553.

Herbst R, Avetisova E, Burden SJ (2002) Restoration of synapse formation in Musk mutant mice expressing a Musk/Trk chimeric receptor. Development 129:5449-5460.

Holland RL, Brown MC (1981) Nerve growth in botulinum toxin poisoned muscles. Neuroscience 6:1167-1179.

Holmes WE, Sliwkowski MX, Akita RW, Henzel WJ, Lee J, Park JW, Yansura D, Abadi N, Raab H, Lewis GD, et al. (1992) Identification of heregulin, a specific activator of p185erbB2. Science 256:1205-1210.

Horsley V, Pavlath GK (2004) Forming a multinucleated cell: molecules that regulate myoblast fusion. Cells Tissues Organs 176:67-78.

Jaworski A, Burden SJ (2006) Neuromuscular synapse formation in mice lacking motor neuron- and skeletal muscle-derived Neuregulin-1. J Neurosci 26:655-661.

Jennings CG, Dyer SM, Burden SJ (1993) Muscle-specific trk-related receptor with a kringle domain defines a distinct class of receptor tyrosine kinases. Proc Natl Acad Sci U S A 90:2895-2899.

Jo SA, Zhu X, Marchionni MA, Burden SJ (1995) Neuregulins are concentrated at nerve-muscle synapses and activate ACh-receptor gene expression. Nature 373:158-161.

Jones G, Meier T, Lichtsteiner M, Witzemann V, Sakmann B, Brenner HR (1997) Induction by agrin of ectopic and functional postsynaptic-like membrane in innervated muscle. Proc Natl Acad Sci U S A 94:2654-2659.

Khanna S, Richmonds CR, Kaminski HJ, Porter JD (2003) Molecular organization of the extraocular muscle neuromuscular junction: partial conservation of and divergence from the skeletal muscle prototype. Invest Ophthalmol Vis Sci 44:1918-1926.

Kummer TT, Misgeld T, Sanes JR (2006) Assembly of the postsynaptic membrane at the neuromuscular junction: paradigm lost. Curr Opin Neurobiol 16:74-82.

Lin W, Burgess RW, Dominguez B, Pfaff SL, Sanes JR, Lee KF (2001) Distinct roles of nerve and muscle in postsynaptic differentiation of the neuromuscular synapse. Nature 410:1057-1064.

Lin W, Dominguez B, Yang J, Aryal P, Brandon EP, Gage FH, Lee KF (2005) Neurotransmitter acetylcholine negatively regulates neuromuscular synapse formation by a Cdk5-dependent mechanism. Neuron 46:569-579.

Lupa MT, Hall ZW (1989) Progressive restriction of synaptic vesicle protein to the nerve terminal during development of the neuromuscular junction. J Neurosci 9:3937-3945.

Matthews-Bellinger J, Salpeter MM (1978) Distribution of acetylcholine receptors at frog neuromuscular junctions with a discussion of some physiological implications. J Physiol 279:197-213.

May P, Herz J (2003) LDL receptor-related proteins in neurodevelopment. Traffic 4:291-301.

McMahan UJ (1990) The agrin hypothesis. Cold Spring Harb Symp Quant Biol 55:407-418.

Meier T, Hauser DM, Chiquet M, Landmann L, Ruegg MA, Brenner HR (1997) Neural agrin induces ectopic postsynaptic specializations in innervated muscle fibers. J Neurosci 17:6534-6544.

Merlie JP, Sanes JR (1985) Concentration of acetylcholine receptor mRNA in synaptic regions of adult muscle fibres. Nature 317:66-68.

Meyer G, Wallace BG (1998) Recruitment of a nicotinic acetylcholine receptor mutant lacking cytoplasmic tyrosine residues in its beta subunit into agrin-induced aggregates. Mol Cell Neurosci 11:324-333.

Misgeld T, Kummer TT, Lichtman JW, Sanes JR (2005) Agrin promotes synaptic differentiation by counteracting an inhibitory effect of neurotransmitter. Proc Natl Acad Sci U S A 102:11088-11093.

Mittaud P, Marangi PA, Erb-Vogtli S, Fuhrer C (2001) Agrin-induced activation of acetylcholine receptor-bound Src family kinases requires Rapsyn and correlates with acetylcholine receptor clustering. J Biol Chem 276:14505-14513.

Morris JK, Lin W, Hauser C, Marchuk Y, Getman D, Lee KF (1999) Rescue of the cardiac defect in ErbB2 mutant mice reveals essential roles of ErbB2 in peripheral nervous system development. Neuron 23:273-283.

Moscoso LM, Chu GC, Gautam M, Noakes PG, Merlie JP, Sanes JR (1995) Synapse-associated expression of an acetylcholine receptor-inducing protein, ARIA/heregulin, and its putative receptors, ErbB2 and ErbB3, in developing mammalian muscle. Dev Biol 172:158-169.

Nitkin RM, Smith MA, Magill C, Fallon JR, Yao YM, Wallace BG, McMahan UJ (1987) Identification of agrin, a synaptic organizing protein from Torpedo electric organ. J Cell Biol 105:2471-2478.

Nguyen TT, Scimeca JC, Filloux C, Peraldi P, Carpentier JL, Van Obberghen E (1993) Co-regulation of the mitogen-activated protein kinase, extracellular signal-related kinase 1, and the 90-kDa ribosomal S6 kinase in PC12 cells. Distinct effects of the neurotrophic factor, nerve growth factor, and the mitogenic factor, epidermal growth factor. J Biol Chem 268:9803-9810.

Ogata T, Yamasaki Y (1988) Scanning electron-microscopic study on the three-dimensional structure of motor endplates of the slow (tonic) muscle fibers in the frog, Rana n. nigromaculata. Cell Tissue Res 252:211-213.

Okada K, Inoue A, Okada M, Murata Y, Kakuta S, Jigami T, Kubo S, Shiraishi H, Eguchi K, Motomura M, Akiyama T, Iwakura Y, Higuchi O, Yamanashi Y (2006) The muscle protein Dok-7 is essential for neuromuscular synaptogenesis. Science 312:1802-1805.

Panzer JA, Song Y, Balice-Gordon RJ (2006) In vivo imaging of preferential motor axon outgrowth to and synaptogenesis at prepatterned acetylcholine receptor clusters in embryonic zebrafish skeletal muscle. J Neurosci 26:934-947.

Panzer JA, Gibbs SM, Dosch R, Wagner D, Mullins MC, Granato M, Balice-Gordon RJ (2005) Neuromuscular synaptogenesis in wild-type and mutant zebrafish. Dev Biol 285:340-357.

Ponomareva ON, Ma H, Vock VM, Ellerton EL, Moody SE, Dakour R, Chodosh LA, Rimer M (2006) Defective neuromuscular synaptogenesis in mice expressing

constitutively active ErbB2 in skeletal muscle fibers. Mol Cell Neurosci 31:334-345.

Porter CW, Barnard EA (1975) The density of cholinergic receptors at the endplate postsynaptic membrane: ultrastructural studies in two mammalian species. J Membr Biol 20:31-49.

Rimer M, Prieto AL, Weber JL, Colasante C, Ponomareva O, Fromm L, Schwab MH, Lai C, Burden SJ (2004) Neuregulin-2 is synthesized by motor neurons and terminal Schwann cells and activates acetylcholine receptor transcription in muscle cells expressing ErbB4. Mol Cell Neurosci 26:271-281.

Ruegg MA, Tsim KW, Horton SE, Kroger S, Escher G, Gensch EM, McMahan UJ (1992) The agrin gene codes for a family of basal lamina proteins that differ in function and distribution. Neuron 8:691-699.

Sandrock AW, Jr., Dryer SE, Rosen KM, Gozani SN, Kramer R, Theill LE, Fischbach GD (1997) Maintenance of acetylcholine receptor number by neuregulins at the neuromuscular junction in vivo. Science 276:599-603.

Schaeren-Wiemers N, Gerfin-Moser A (1993) A single protocol to detect transcripts of various types and expression levels in neural tissue and cultured cells: in situ hybridization using digoxigenin-labelled cRNA probes. Histochemistry 100:431-440.

Sohal GS (1988) Development of postsynaptic-like specializations of the neuromuscular synapse in the absence of motor nerve. Int J Dev Neurosci 6:553-565.

Srihari T, Vrbova G (1978) The role of muscle activity in the differentiation of neuromuscular junctions in slow and fast chick muscles. J Neurocytol 7:529-540.

Thaler J, Harrison K, Sharma K, Lettieri K, Kehrl J, Pfaff SL (1999) Active suppression of interneuron programs within developing motor neurons revealed by analysis of homeodomain factor HB9. Neuron 23:675-687.

Traverse S, Gomez N, Paterson H, Marshall C, Cohen P (1992) Sustained activation of the mitogen-activated protein (MAP) kinase cascade may be required for differentiation of PC12 cells. Comparison of the effects of nerve growth factor and epidermal growth factor. Biochem J 288 (Pt 2):351-355.

Valenzuela DM, Stitt TN, DiStefano PS, Rojas E, Mattsson K, Compton DL, Nunez L, Park JS, Stark JL, Gies DR, et al. (1995) Receptor tyrosine kinase specific for the skeletal muscle lineage: expression in embryonic muscle, at the neuromuscular junction, and after injury. Neuron 15:573-584.

Vogel Z, Sytkowski AJ, Nirenberg MW (1972) Acetylcholine receptors of muscle grown in vitro. Proc Natl Acad Sci U S A 69:3180-3184.

Wallace BG (1991) The mechanism of agrin-induced acetylcholine receptor aggregation. Philos Trans R Soc Lond B Biol Sci 331:273-280.

Wang ZZ, Washabaugh CH, Yao Y, Wang JM, Zhang L, Ontell MP, Watkins SC, Rudnicki MA, Ontell M (2003) Aberrant development of motor axons and neuromuscular synapses in MyoD-null mice. J Neurosci 23:5161-5169.

Weatherbee SD, Anderson KV, Niswander LA (2006) LDL-receptor-related protein 4 is crucial for formation of the neuromuscular junction. Development 133:4993-5000.

Witzemann V (2006) Development of the neuromuscular junction. Cell Tissue Res 326:263-271.

Woldeyesus MT, BritSCh S, Riethmacher D, Xu L, Sonnenberg-Riethmacher E, Abou-Rebyeh F, Harvey R, Caroni P, Birchmeier C (1999) Peripheral nervous system defects in erbB2 mutants following genetic rescue of heart development. Genes Dev 13:2538-2548.

Wolpowitz D, Mason TB, Dietrich P, Mendelsohn M, Talmage DA, Role LW (2000) Cysteine-rich domain isoforms of the neuregulin-1 gene are required for maintenance of peripheral synapses. Neuron 25:79-91.

Yang X, Li W, Prescott ED, Burden SJ, Wang JC (2000) DNA topoisomerase IIbeta and neural development. Science 287:131-134.

Yang X, Arber S, William C, Li L, Tanabe Y, Jessell TM, Birchmeier C, Burden SJ (2001) Patterning of muscle acetylcholine receptor gene expression in the absence of motor innervation. Neuron 30:399-410.

Zhao H, Nonet ML (2000) A retrograde signal is involved in activity-dependent remodeling at a C. elegans neuromuscular junction. Development 127:1253-1266.

Zuo Y, Lubischer JL, Kang H, Tian L, Mikesh M, Marks A, Scofield VL, Maika S, Newman C, Krieg P, Thompson WJ (2004) Fluorescent proteins expressed in mouse transgenic lines mark subsets of glia, neurons, macrophages, and dendritic cells for vital examination. J Neurosci 24:10999-11009.

Vita

Vita Marie Vock was born in Elgin, Illinois on April 25, 1963. She is the second daughter of Freda Grace (Taylor) Vock and Robert Edward Vock. After graduating from Santa Fe Christian High School in Solana Beach, California, she attended San Diego Mesa College for 3 semesters before leaving school and devoting herself to full-time parenting. In 1990, she returned to baccalaureate studies at Moorpark Community College in Moorpark, California, transferring to The University of Nebraska in Lincoln, Nebraska in 1993. She received the Bachelor of Science in Biochemistry from The University of Nebraska in 1998. During the following years she was employed as a Research Assistant in laboratories at the M.D. Anderson Cancer Center in Houston, Texas and at The University of Texas in Austin, Texas. In August of 2001 she entered the Graduate School of The University of Texas, at the Lyndon Baines Johnson School of Public Affairs. She completed coursework requirements for the Masters of Public Affairs, and in the fall of 2003 she transferred into the Doctoral Program in Neuroscience.

Permanent Address: 944 Grayson Lane, Charlottesville, Virginia, 22903
This dissertation was typed by the author